Canatec Associates International Ltd.

POLYNYAS IN THE CANADIAN ARCTIC

Analysis of MODIS Sea Ice Temperature Data Between June 2002 and July 2013

David Currie

7/16/2014

Using daily sea ice temperature grids produced from MODIS optical satellite imagery, polynya occurrences in the Canadian Arctic and Northwest Greenland were mapped with a spatial resolution of one square kilometer and a temporal resolution of one week. The eleven year dataset was used to identify and measure locations with a high probability of open water occurrence. This approach appears to be most suitable for the spring months, when polynyas and shore leads represent the only open water in the region. An analysis of the results at several geographic scales reveals considerable yearly variation in polynya extents, although the relatively short period studied makes identifying trends rather difficult.

Contents

POLYNYAS IN THE CANADIAN ARCTIC

Analysis of MODIS Sea Ice Temperature Data Between June 2002 and July 2013
For WWF Global Arctic Programme
Prepared by: David Currie, P.Eng.
Canatec Associates International Ltd.
July 16, 2014

Introduction

This is one of a series of research resources commissioned by WWF to help inform future management of the Area we call the Last Ice Area. We call it that because the title refers to the area of summer sea ice in the Arctic that is projected to last. As climate change eats away at the rest of the Arctic's summer sea ice, climate and ice modelers believe that the ice will remain above Canada's High Arctic Islands, and above Northern Greenland for many more decades.

Much life has evolved together with the ice. Creatures from tiny single celled animals to seals and walrus, polar bears and whales, depend to some extent on the presence of ice. This means the areas where sea ice remains may become very important to this ice-adapted life in future.

One of my colleagues suggested we should have called the project the *Lasting* Ice Area. I agree, although it's a bit late to change the name now, that name better conveys what we want to talk about. While much is changing, and is likely to change around the Arctic, this is the place that is likely to change the least. That is also meaningful for the people who live around the fringes of this area – while people in other parts of the Arctic may be forced to change and adapt as summer sea ice shrinks, the people around the LIA may not have to change as much.

As a conservation organization, WWF does not oppose all change. Our goal is to help maintain important parts of the natural world, parts that are important just because they exist, and important for people. WWF does not have the power and authority to impose its vision on people. Instead, we try to present evidence through research, and options for action. It is then up to the relevant authorities as to whether they will take action or not; the communities, the Inuit organizations, and the governments of the Last Ice Area will decide its future fate. We hope you will find the information in these reports useful, and that it will help you in making wise decisions about the future of the Last Ice Area.

Clive Tesar, Last Ice Area lead.

Polynyas and the Last Ice Area

This report flows from a workshop on the Last Ice Area held in Iqaluit, Nunavut in summer 2013. Several Inuit at the workshop referred to polynyas, their importance, and their concerns about what might happen to polynyas in a changing global climate. The importance of polynyas in the Arctic is quite well researched. As noted by Karnovsky et al (2007) "The distribution of most bird and mammal colonies in the Arctic and in turn the villages (especially prehistoric ones) of the hunter gatherer native peoples *Homo sapiens,* is strongly related to the presence of polynyas." In other words, not only are many Arctic birds and mammals strongly dependent on polynyas, but the communities of Arctic peoples are where they are in many cases because of the concentrations of wildlife around those polynyas, providing food for people in those communities. In terms of their significance to wildlife, a main function is to provide wintering areas for Arctic-wintering birds such as some species of eider ducks, and to provide food for early-nesting migrant seabirds (Meltofte, 2013).

The problem in responding to the questions and concerns raised in the Iqaluit Last Ice Area workshop is that, in the words of Tynan and DeMaster (1997) "…predictions of the occurrence, location, and productivity of polynyas in a warmer Arctic are unavailable." This report does not answer all of those questions, it is intended however to make a start at answering them. This start (as described in more detail in the report introduction) is intended to further knowledge of the existing size and duration of larger polynyas within the Last Ice Area, and to see if there were any trends in the polynyas' size or duration. We hope that this may help in a future effort to model the persistence of the region's polynyas.

A polynya is an area of open water which may occur in normally ice-covered regions due to the effects of wind, currents, or upwelling warm water. (Canadian Ice Service, 2011) The unique factors that preserve these features through the winter season have been studied in some depth. In the Canadian Archipelago, tidal models have been used to predict polynya formation but this approach is limited by the quality of available bathymetry and current data and does not account for polynyas formed by the wind. (Hannah, 2009)
According to the World Meteorological Organization standard nomenclature, several types of polynya are described:

> 7.4 Polynya: Any non-linear shaped opening enclosed in ice. Polynyas may contain brash ice and/or be covered with new ice, nilas or young ice.
> 7.4.1 Shore polynya: A polynya between drift ice and the coast or between drift ice and an ice front.
> 7.4.2 Flaw polynya: A polynya between drift ice and fast ice.
> 7.4.3 Recurring polynya: A polynya, which recurs in the same position every year.

An inventory of 23 recurring polynyas in the Canadian Arctic are described in Barber and Smith, 2007. The polynyas were identified using traditional knowledge supplemented with the Polynya Signature Simulation Method (Markus and Burns, 1995), a well developed technique which classifies open water, thin ice, and thick ice based on polarization ratios of DMSP microwave imagery. Although the resolution of the source dataset is 15 km, the sub-pixel analysis results have a nominal spatial resolution of 6.25 km.
The purpose of this project was to expand on previous studies using daily MODIS satellite

image data to detect polynya with high spatio-temporal frequency over the period July 2002 to June 2013. The project area covers the region outlined in figure 1,

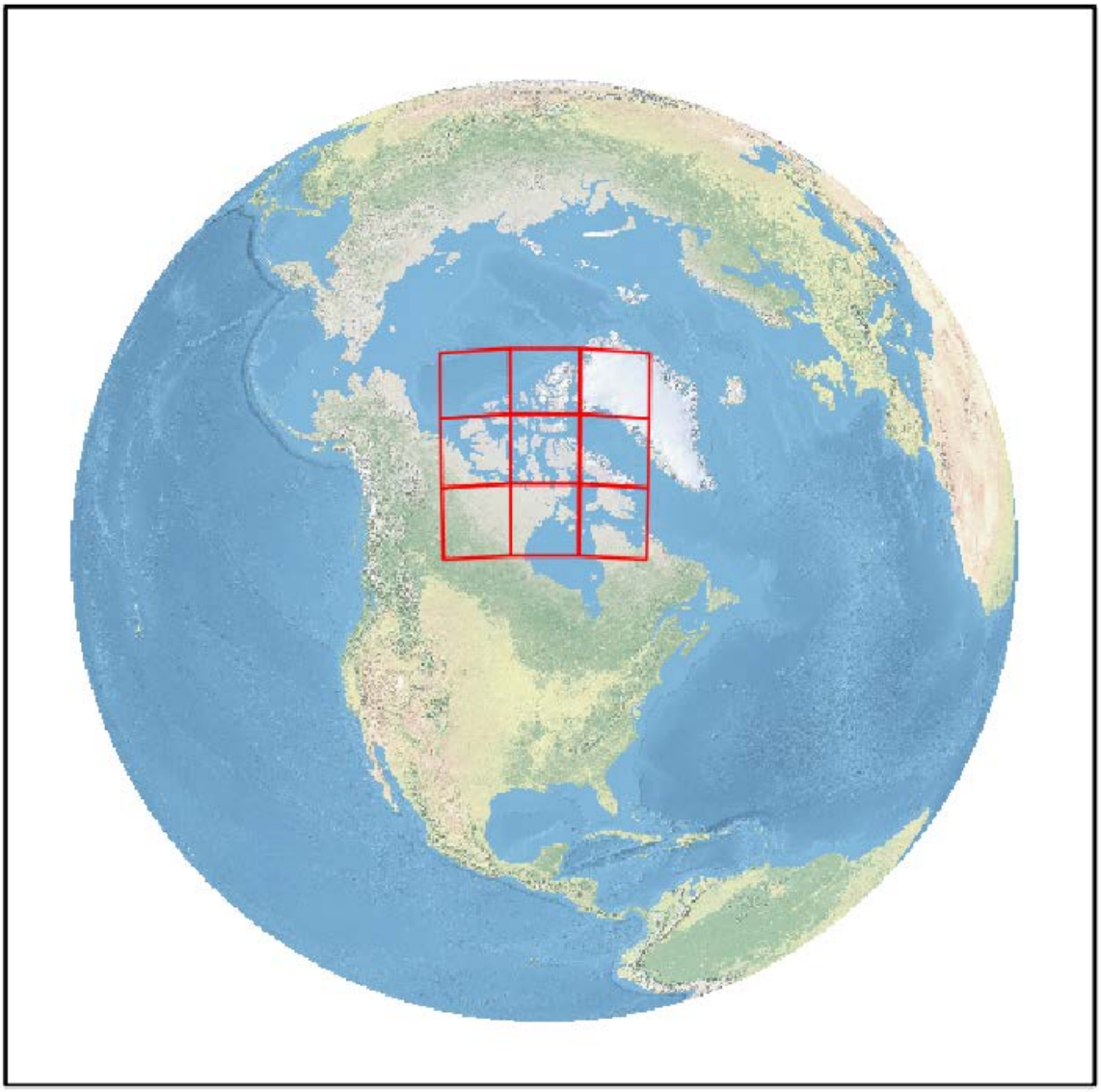

Figure 1: Project Location: The MODIS Ice Temperature data used for this project is archived in tiles arranged around the North and South poles. The nine tiles depicted were selected to cover the Canadian Archipelago, Northwest Greenland, and the Northern portions of Baffin and Hudson Bays.

Goals

Using higher resolution MODIS imagery, detection of small polynyas and accurate estimates of area should be possible, although the effects of cloud may reduce the frequency of

available observations. The objectives of the present study are to:
* Identify and locate polynya features occurring in the Canadian Arctic and Northwest Greenland over the past decade
* Compare with earlier data
* Identify trends within the results

Source Data

The primary data used for this project is the sea ice temperature grid product MOD29/MYD29 produced using the Moderate Resolution Imaging Spectrometer (MODIS) instrument carried aboard the Terra and Aqua polar orbiting satellites. This dataset has a spatial resolution of 1 km. The use of MODIS data provides high temporal frequency at moderate resolution and low cost. This data has been used with some success for detecting polynya and observing daily fluctuations in their extents, Clappa and Budillon 2012.

MODIS Sea Ice Temperature Product MOD29/MYD29

Produced daily using multiple passes, there are night and day grids produced for each satellite with the following designations:

Satellite	Terra	Aqua
Daytime	MOD29P1D	MYD29P1D
Nighttime	MOD29P1N	MYD29P1N

Spatially, the MOD29 data are produced in an array of tiles with a Lambert azimuthal equal area projection centered on the pole. Not all of these grids are available for all days, since depending upon latitude and date there may be no day or night periods. In both day and night cases, the sea ice temperature is estimated for each one square kilometer cell using a split window algorithm applied to thermal infrared bands at wavelengths of 11.03mm and 12.02mm. Land and cloud masks are used to remove non-seaice cells. Temperatures are expressed in degrees Kelvin with a precision of 0.01°. The daytime products also include a sea ice by reflectance grid, which identifies sea ice and open water using ratios of visible and near infrared observations. These grids indicate only presence/absence of ice or water and are only available when the location is sunlit. While the reflectance grids were unavailable during the critical winter periods, these data proved to be essential for obtaining a good result during the summer melt season, as water ponds on the ice pack are indistinguishable from open water using temperature readings alone.
Appendix A provides a discussion of the algorithms and processing used to produce the MOD29 dataset.

Landsat Quicklook Imagery

Data from the Landsat series of satellites provides a useful screening tool for algorithm development and validating the results of the MOD29 processing. There are several thousand images available in the project area during the 2002-2013 time period, although

they are mainly restricted to the March-October time frame and do not provide the broad regional coverage as MODIS. Rather than download the full scene imagery, quicklook data available online is suitable for comparison at small scales and several hundred of these scenes were used in this project. The quicklooks were obtained from the NASA Global Visualization Viewer at http://glovis.usgs.gov.

Canadian Ice Service Charts

Daily and weekly ice charts produced by the Canadian Ice Service, primarily from Radarsat imagery, are available with suitable scale for identifying larger polynya features, however in practice these features are rarely mapped as such. A selection of weekly regional ice charts for the Western and Eastern Arctic were obtained for the project area, but did not prove useful for this work.

Methods

Data Management

MOD29/MYD29 gridded data were downloaded from the National Snow and Ice Data Center (NSDIC) in Boulder Colorado. The data grids are organized by date and subdivided into tiles, each covering roughly 100,000 square kilometers with a one kilometer grid spacing. As shown in figure 1, the project area is covered by nine tiles. For each day, there is a possibility of four data grids, representing Day and Night results from the Aqua and Terra satellites. For the project time frame of 4017 days, this gives a maximum of 144612 possible data grids, however not all datasets were available. The temporal distribution of these grids is illustrated in figure 2.

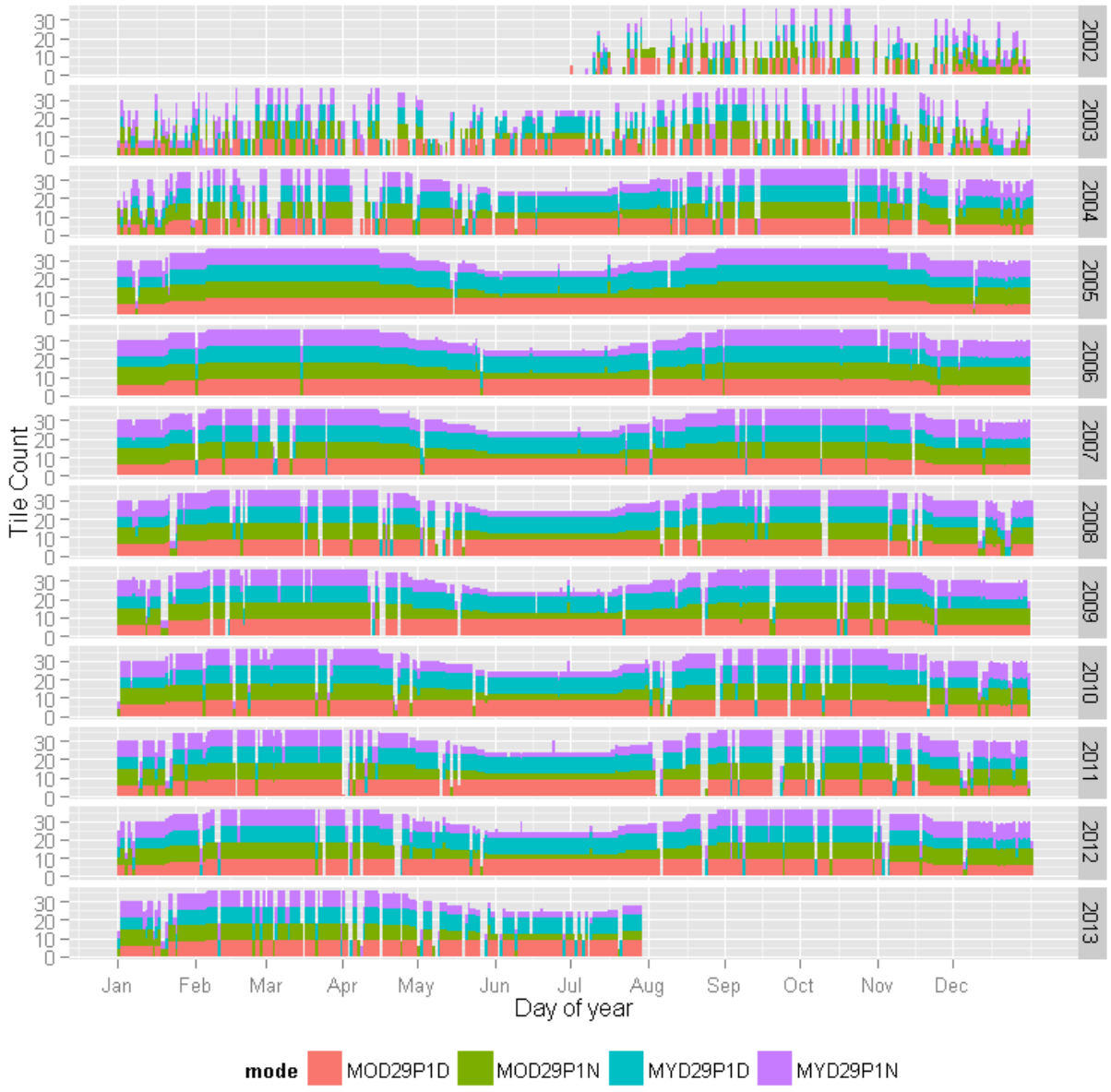

Figure 2: Temporal Distribution of Raw Data Grids: Each bar represents one day within the project timeframe. The height of the bar indicates the number of available MOD29 grid tiles available for that day. The color indicates the type. The project area covers nine tiles, so for the four different types there are a maximum of 36 possible tiles available each day.

A total of 110678 grid tiles are represented. Over the 4017 total days in the project time frame, data is available for 3872 days although there are many missing data values within the grids either because of cloud, sensor problems, or limitations of the MOD29 data processing algorithm. As illustrated in the figure, the data available from the early years (2002-2003) is somewhat inconsistent, with many missing tiles. The cause of the missing data may be related to sensor calibration problems or issues with the MOD29 algorithm, which was revised several times over the past decade. In any case, there are many data gaps in the early records and for this reason a start date of July 2002 was selected for this

project in order to ensure that a sufficient number of observations was available to prepare a continuous thematic coverage of the project area.

For the data processing task, the volumes of data were aggregated into separate files spanning 365 or 366 days, to accommodate leap years. Although some polynyas may be evident in any season, most are indistinguishable from the surrounding environment during the summer. For these seasonal polynyas, the natural time frame begins in the fall during freeze-up and ends in the spring, when the polynyas act as seed points from which the break-up expands. To accommodate seasonal analysis, the grids were grouped by date into eleven seasonal arrays spanning the range of July 1 to June 30 so that the critical winter period was in the center of each group.

For efficient data storage, while still accomodating missing data, the incoming sea ice temperature grids were combined into multilayer raster files containing all the data for a single tile for each mode collected within a single year. These 594 files were used as the source for the classification process.

Classification

All of the data processing was performed using the Geospatial Data Abstraction Layer (GDAL) and RASTER software libraries, under the control of the R scripting environment. For all of the data grids, the sea ice temperature results were classified into the following classes:

Class	Observation
1	Cloud
2	Ice < 268°K
3	Ice < 269°K
4	Ice < 270°K
5	Ice < 271°K
6	Ice < 272°K
7	Ice < 273°k
8	Open Water (273°K)

In addition, for the daytime data grids, the reflectance results were classed as:

Class	Observation
1	Cloud
2	Sea Ice
8	Open Water

Any readings not falling into these classes were discarded. In the best case scenario, when both day and night grids were available from the Terra and Aqua satellites, a total of six observations for each one square kilometer grid cell are provided for the day. Roughly two thirds of the project area lies north of the arctic circle, where the maximum number of

observations is only obtained in the spring and fall seasons, when both day and night time conditions occur.

Aggregation

Two data aggregation steps were performed in order to maximize the desired open water/sea ice signal and minimize the cloud readings, resulting in composite grids representing daily and weekly intervals.

The first aggregation step was to stack all of the available data grids for each day using a filter biased to open water and warmer sea ice. The result of this process is a set of data grids for each day in which data are available. The filter used to select the final value for a grid cell from among up to six observations is a maximum value choice based on the classification scheme given above. The single exception to this rule is in the case where a daytime reflectance observation indicates ice while the temperature observation indicates open water (273°K). This situation is consistent with melt ponds on the ice surface, and so the final value is set to 2, indicating ice. Figure 3 shows an example for a single day, where the classified results from the various daily grids are shown along with the aggregated result - referred to from here on as a Daily Open Water Composite Grid.

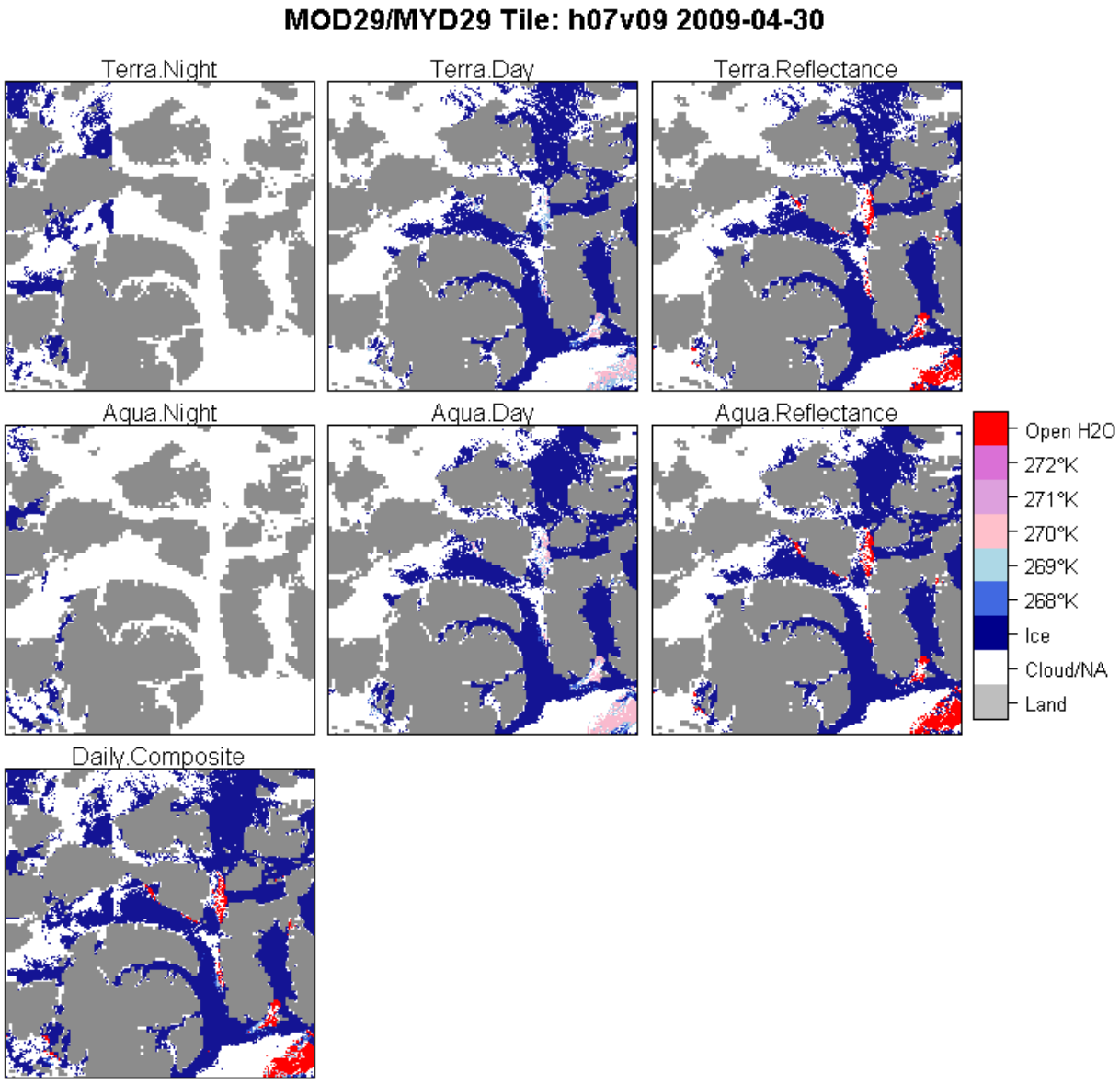

Figure 3: Classified Daily Grids: Example from a single date showing the six MOD29 grids available. Note the areas of no data (white) resulting from continous sunlight in the northern portion. The Daily Open Water Composite at bottom left is an aggregated result, which illustrates how the multiple classifications are combined in order to preserve the open water signal. A single tile is shown, north is to the right in the presentation.

Note that these grids are shown in the default Lambert azimuthal equal area projection and that North is to the right in this view.
The above figure illustrates a few important issues regarding the day and night versions of the MOD29 product and how the data vary with date. Noting that the selected scene is from April 30, the night time grids are only half populated due to continuous sunlight at the more northerly latitudes.
The Daily Open Water Composite grids produced in the first aggregation step still contain

considerable amounts of cloud and of course there are missing dates in the coverage. In order to produce a low-cloud estimate with a continuous time frequency, a second aggregation step was performed in which multiple days were combined, using the maximum value favoring open water/warm ice values, resulting in a set of data grids representing weekly time spans, these grids will be referred to as Weekly Open Water Composites.

Results

Daily Open Water Composites

A total of 3872 grids at 1km resolution were created from the classification phase. Dates for which no data were available were skipped. The results do not represent continuous thematic coverages due to missing input tiles and cloud. Figure 4 shows one tile of this data over seven days, with the aggregated weekly result included as the last tile in the group. Note that the week shown in the example is represented by only 6 days due to missing input data.

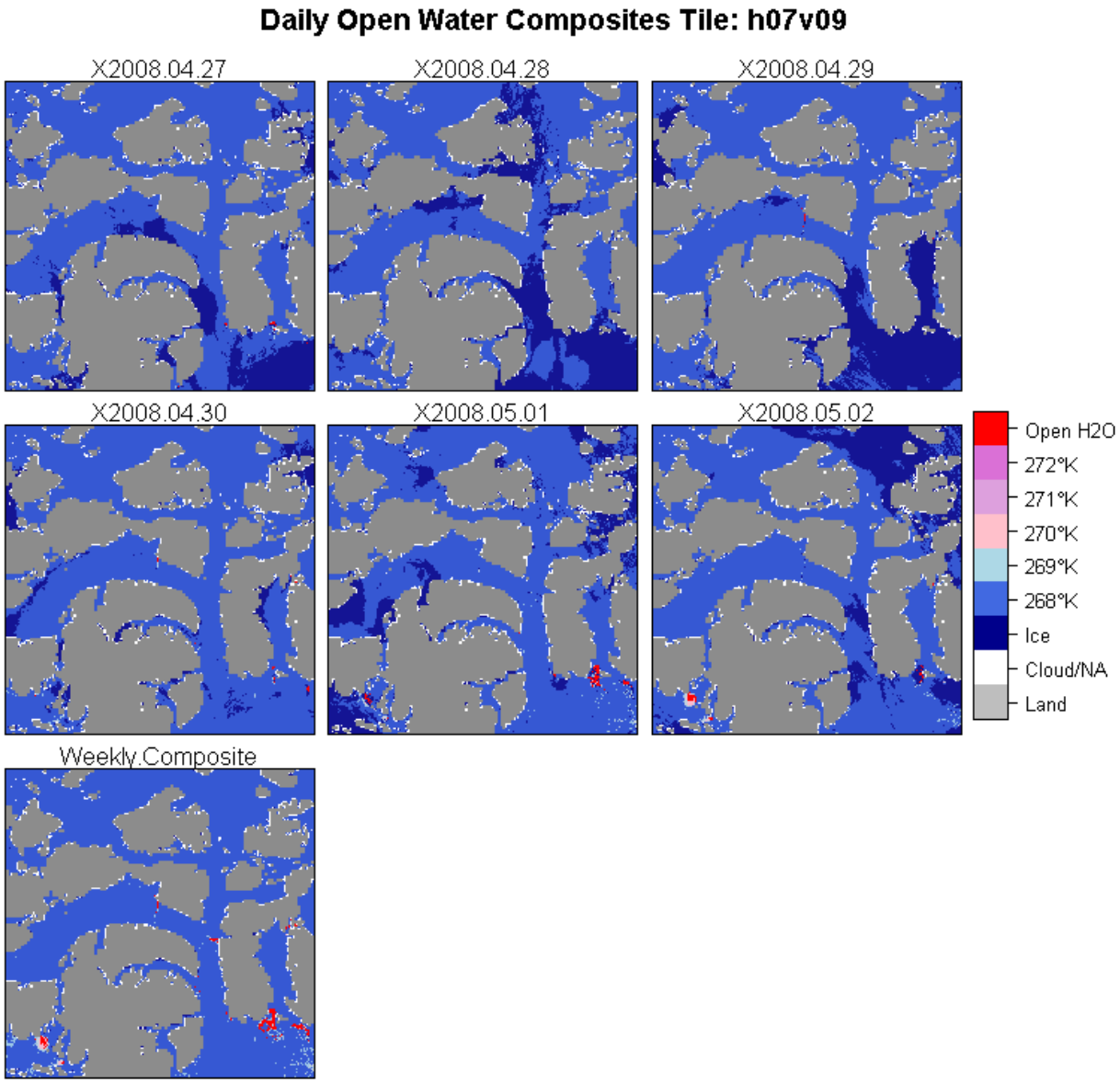

Figure 4: Daily Open Water Composites April 27-May 02, 2008: Example of Daily Open Water Composite grids over the span of a single week showing how the occurance of open water fluctuates over the period. The Weekly Open Water Composite shown in the lower left shows how seven daily grids are combined to produce a weekly result which preserves the open water signal. In the week shown, only six days of data were available. A single tile is shown, north is to the right in this presentation.

For a more detailed view from a different time period, figure 5 shows a similar set of views zoomed into the Devon Island region. In this case, the input data includes a complete set of 7 days.

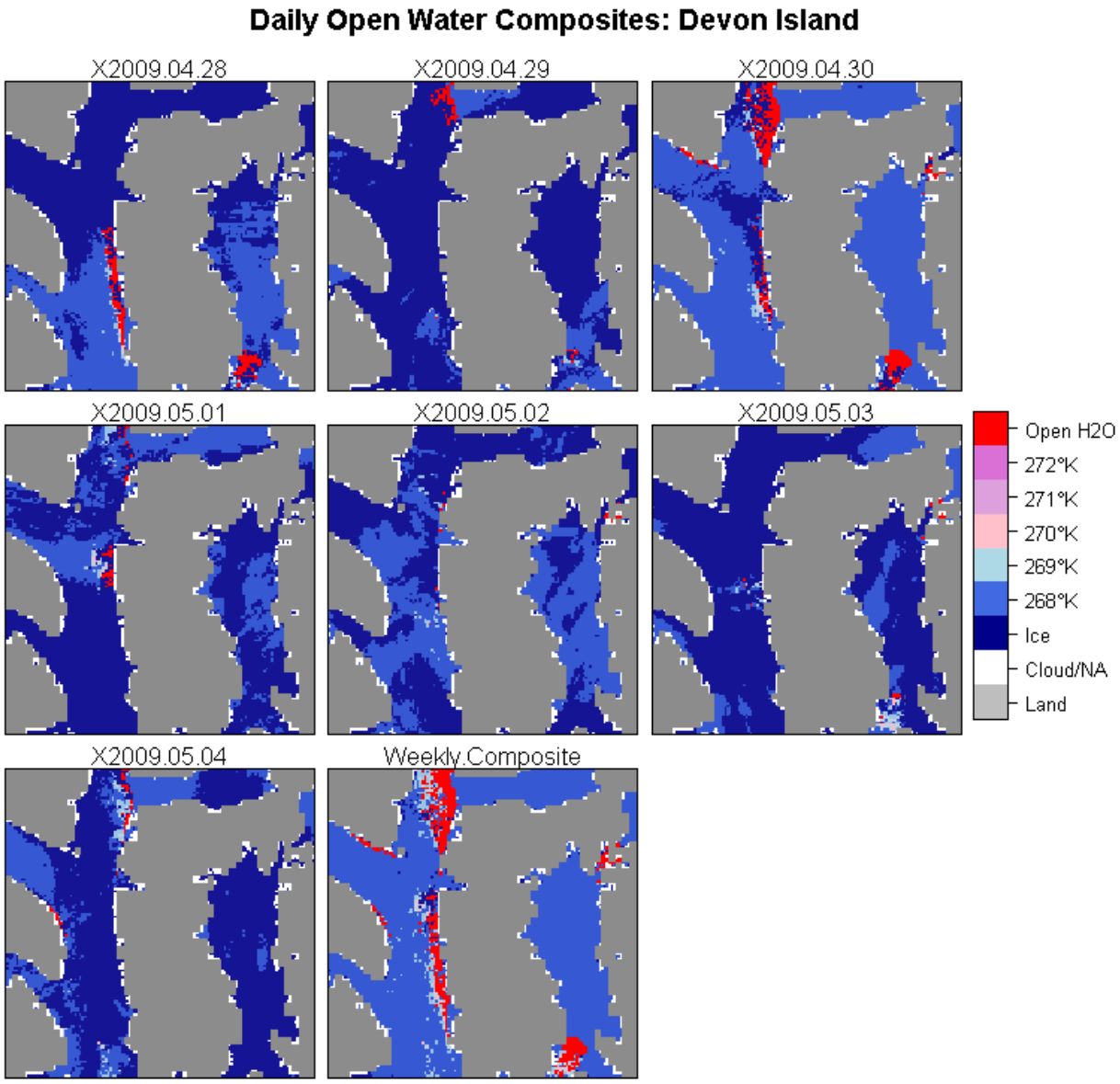

Figure 5: Daily Open Water Composite Close Up April 28 -May 04, 2009: As with the previous figure, Daily Open Water Composite grids are shown for a one week span. Note the open water signals (red) which flutuate through the period. The aggregation process used to produce the Weekly Open Water Composite grid, at bottom center, preserves all of the open water signals. For the week shown, all seven days are represented. North is to the right in this presentation.

Weekly Open Water Composites

There are 572 Weekly Open Water Composite grids containing aggregated, classified values at 1km resolution. Figure 6 shows an example for one seven day period over the entire project area using a polar stereographic projection (North up). The projection will be used

for the remainder of this report in order to present maps with a familiar appearance.

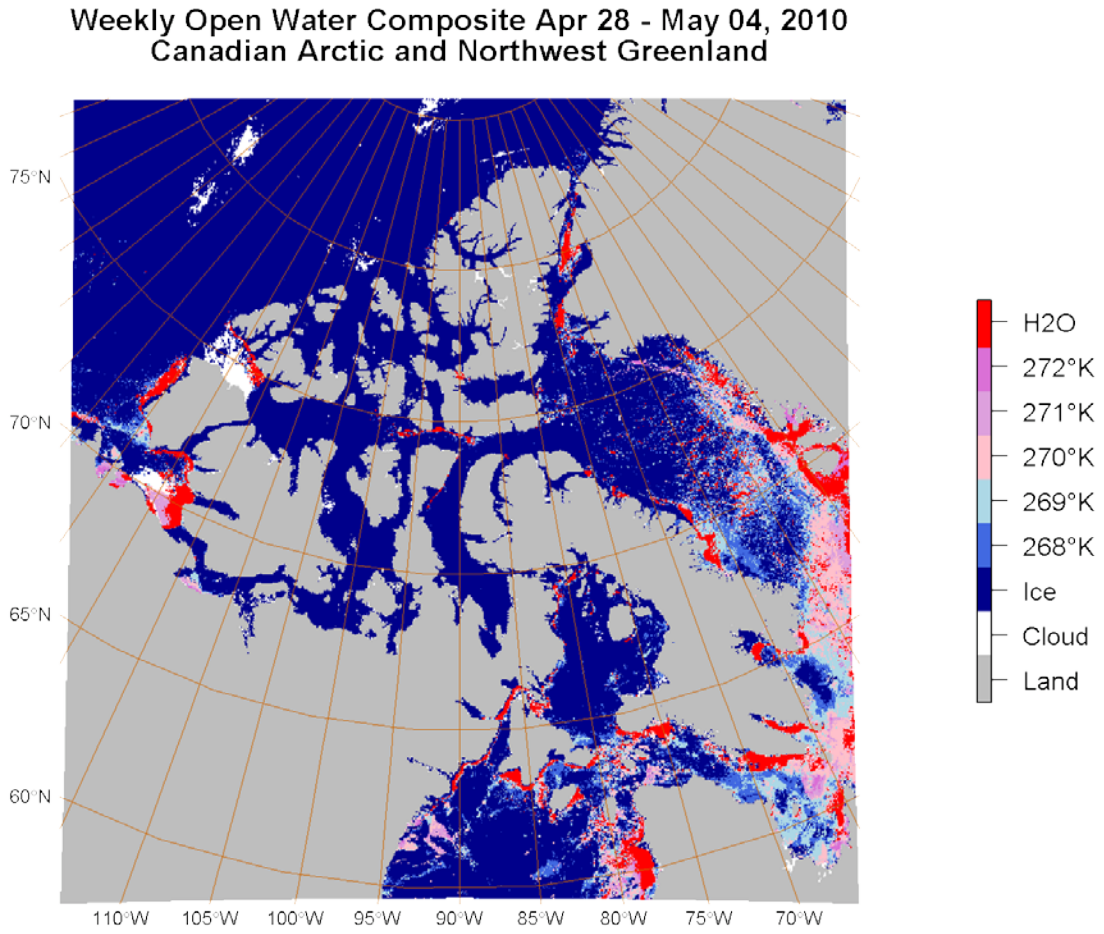

Figure 6: Weekly Open Water Composite April 28-May 04, 2010: Example from a single week showing the entire project extent. The one kilometer resolution grid represents an aggregation of seven Daily Open Water Composite grids using a filter which preserves any open water observations. Note that even with a possible 42 observations for each grid cell, some areas are classified as cloud, shown in white.

And here is a more detailed view of the Devon Island region.

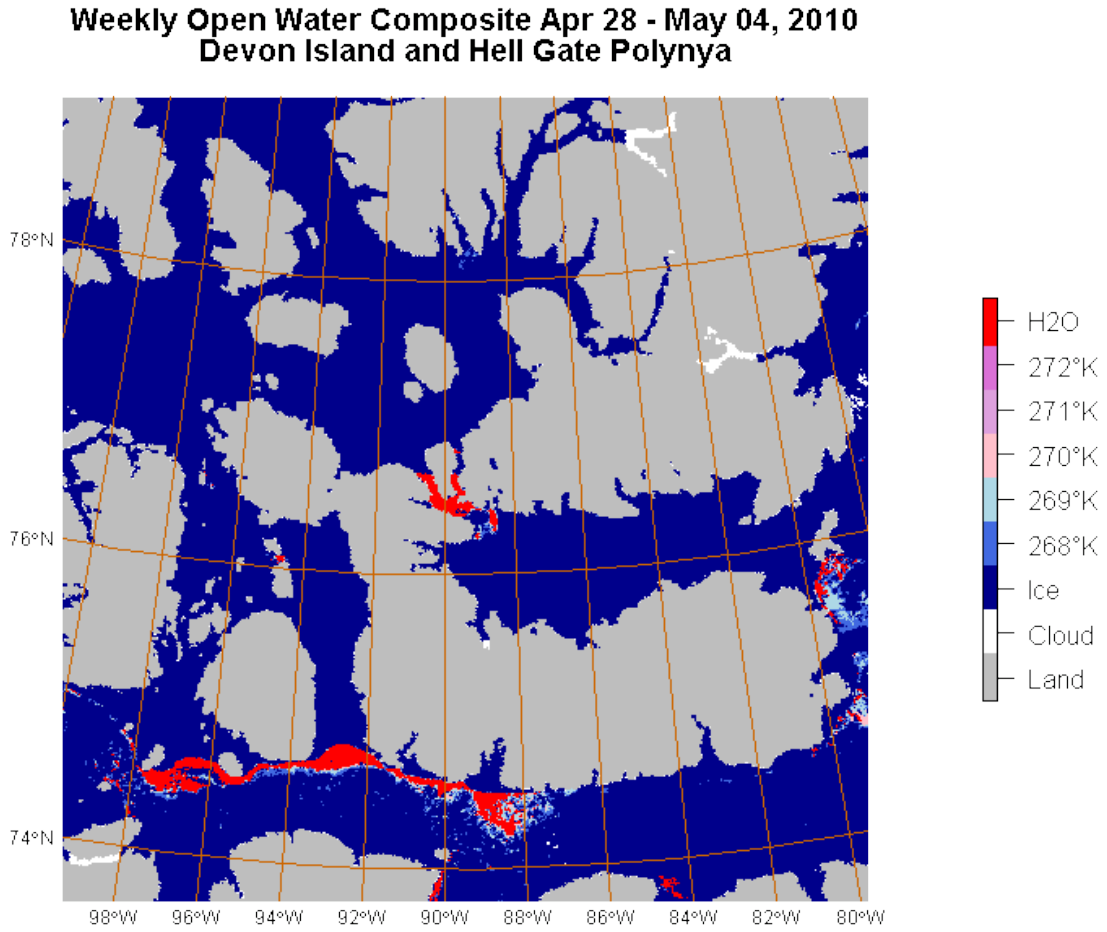

Figure 7: Weekly Open Water Composite Close UpApril 28-May 04, 2010: As with the previous figure, this figure shows the result for a single week, centered on Devon Island. Several well known polynyas are evident, including large areas of open water in Lancaster Sound and Hell Gate.

A complete set of the weekly open water composite grids may be viewed in Appendix B.

Weekly Empirical Probability of Occurrence Grids

Using the weekly open water composite grids, a spatial estimate of the probability of occurrence for open water was created with a four kilometer grid spacing. The four kilometer grid spacing was selected in order to ensure a sufficient sample population was available for each grid cell, since any cloud readings were treated as no data. The empirical probability of occurrence (EPO) for an individual grid cell is calculated as the count of all open water pixels observed within the four kilometer cell during the week in question for all years, divided by the count of all open water and ice pixels observed in the same period.

$$EPO \quad = \frac{N_{H_2O}}{N_{H_2O} + N_{Ice}}$$

Note that cloud readings are excluded from the computation. Using a 4km spacing over the eleven year period, the maximum value of *i* is 176. Figure 8 shows a graphical representation of the EPO grid for one week,

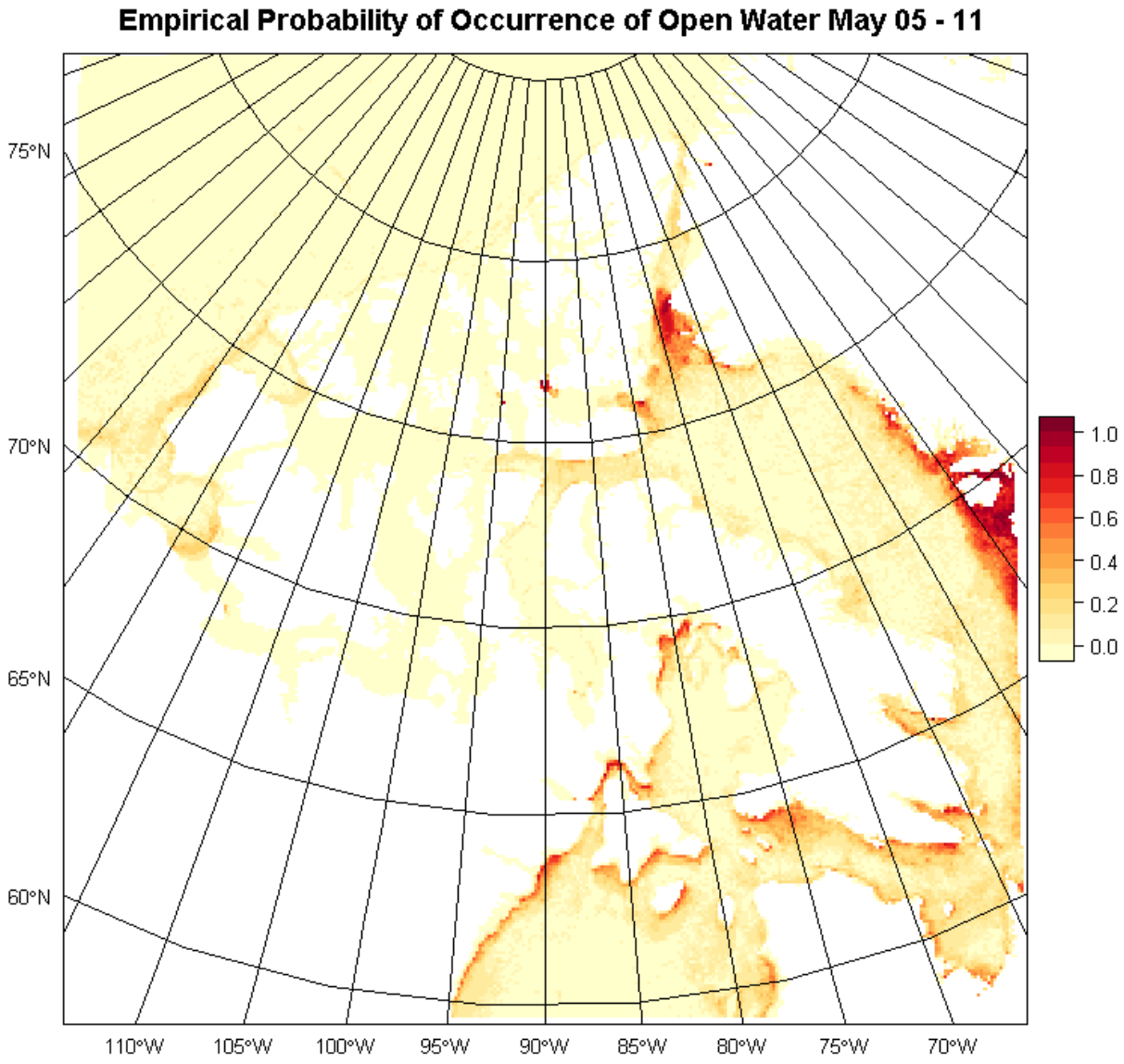

Figure 8: Probability of Occurrence - All Years: This 4km grid represents the probability of open water during the seven day time period indicated. The values are calculated from the weekly open water composite grids.

while figure 9 shows a detailed view of the Devon Island region.

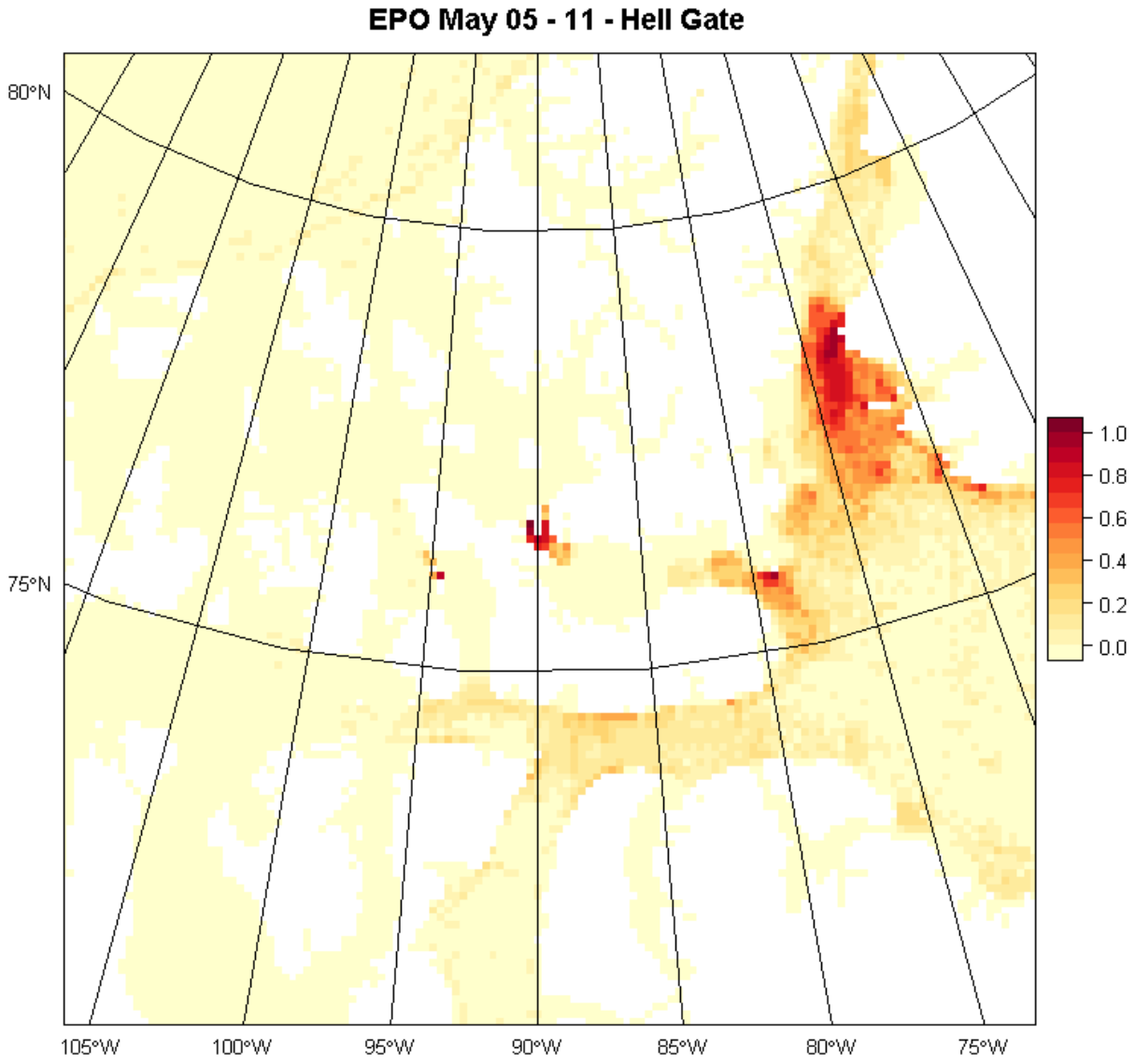

Figure 9: Probability of Occurrence Close Up - All Years: As with the previous figure, this grid represents the calculated probability of open water around Devon Island for the time period noted. The polynyas at Dundas Is., Hell Gate, Lady Ann Strait, and North Water are clearly indicated, with probability values greater than 0.8.

The complete set of EPO grids for all 52 weeks are available in Appendix C.

Quality Assessment and Error Sources

Spatial and temporal sensitivity

In order to validate the results of the classification, 397 Landsat quicklook images were obtained and compared with the corresponding result. The Landsat quicklooks are produced using visible and near infrared bands at a resolution of 180m which is a very useful presentation for this application. Since the images are at a significantly higher resolution than the MODIS data small features that may be poorly sensed by MODIS are evident. Open water has a characteristic dark tone, while ice and cloud are white and blue. The following figures provide a few examples of the comparison.

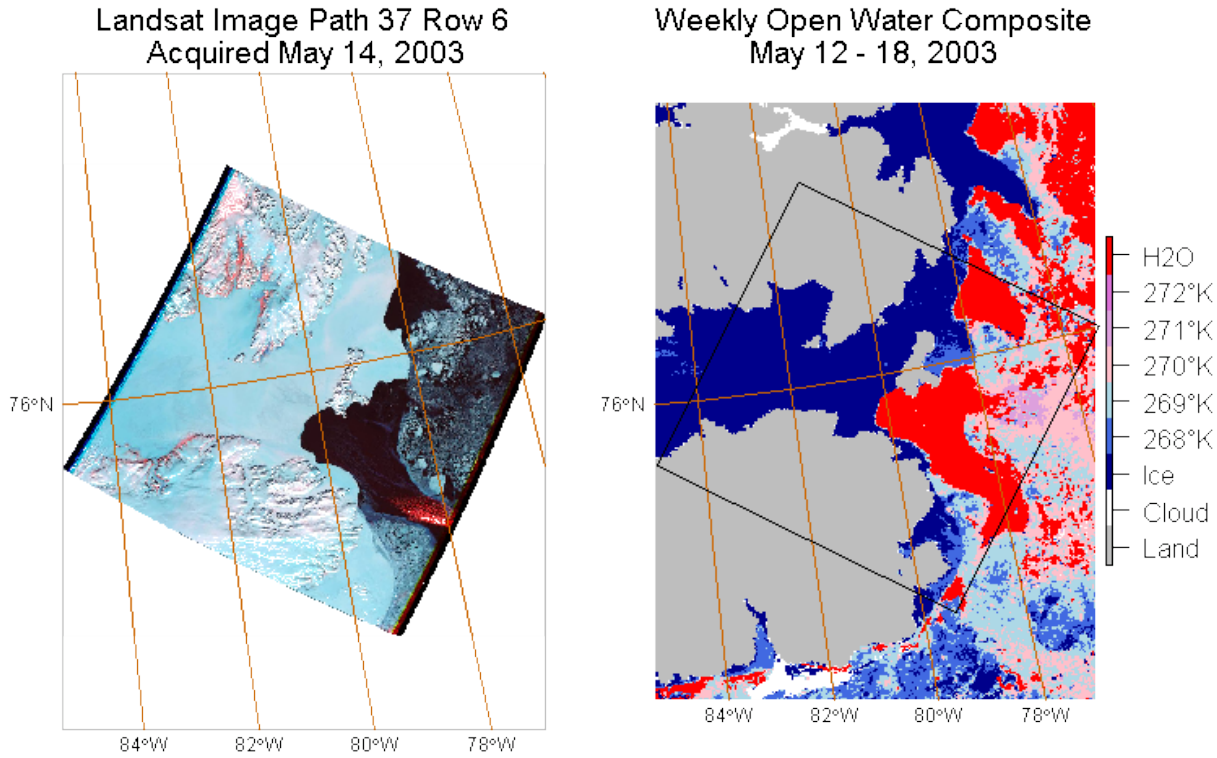

Figure 10: Landsat Comparison - Coburg Island 2003

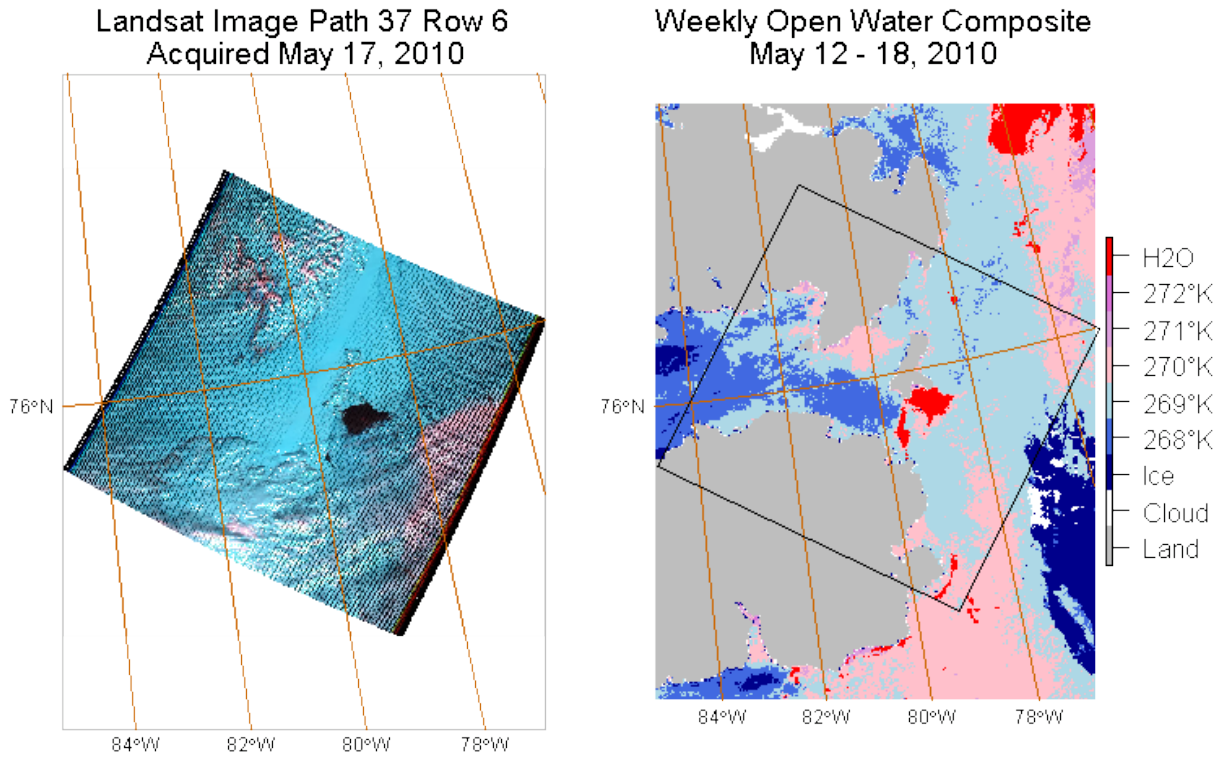

Figure 11: Landsat Comparison - Coburg Island 2010

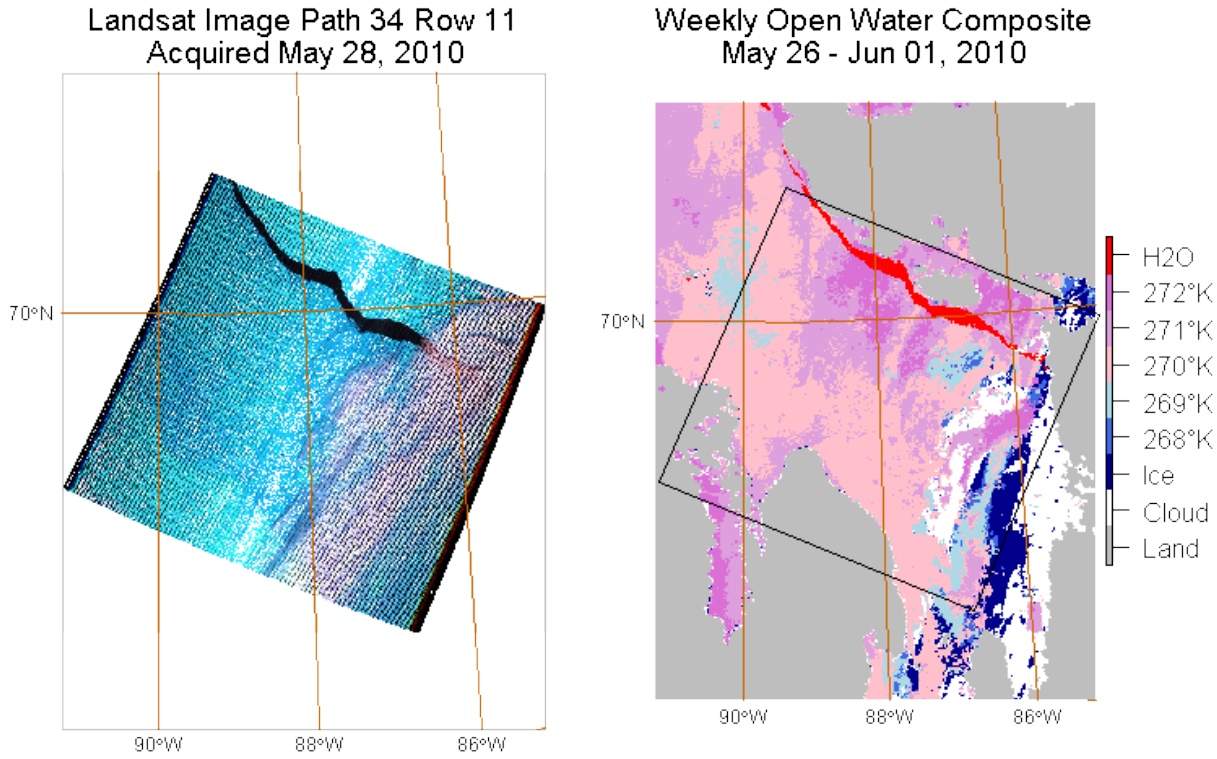

Figure 12: Landsat Comparison - Committee Bay 2011

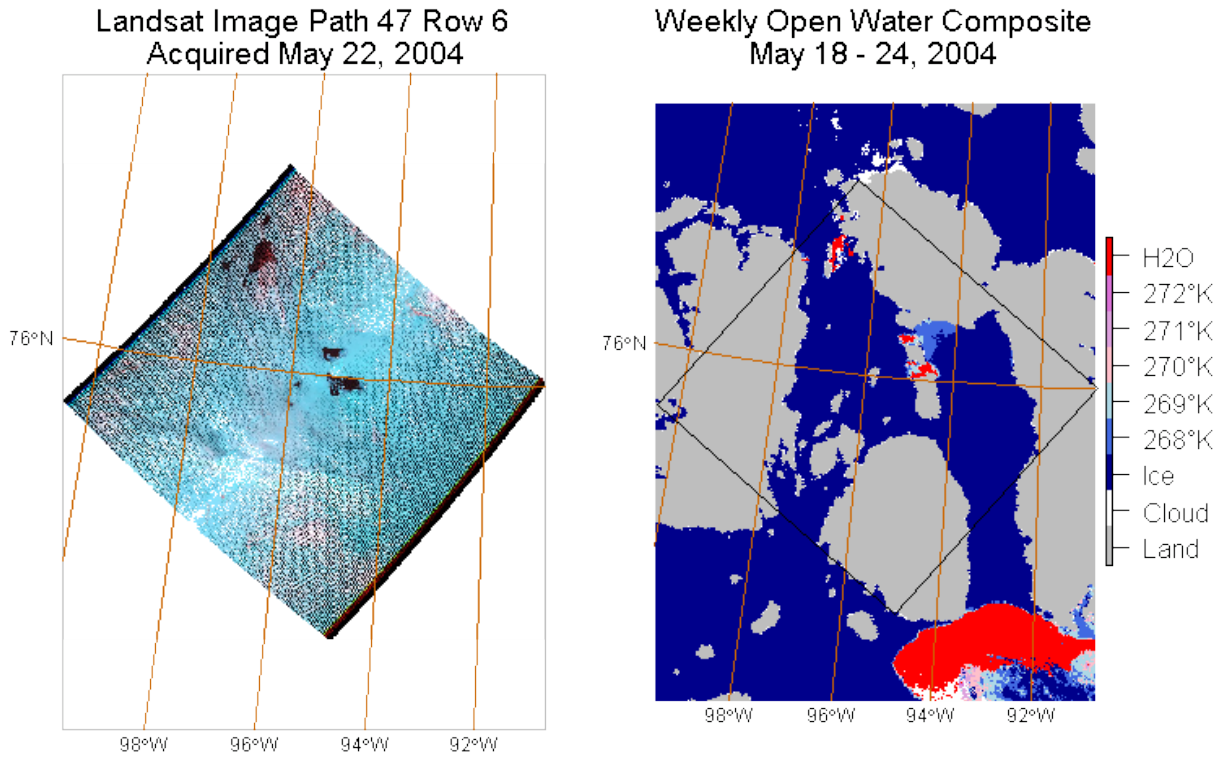

Figure 13: Landsat Comparison - Dundas Island 2004

A visual assessment of the correspondence between the Landsat and Weekly Open Water Composite grids was performed in order to identify potential errors in the analysis and guide the interpretation of the results. The full set of images used may be reviewed in Appendix D.

Persistent Cloud Cover

In the winter season, the interaction of open water and cold air will result in the formation of cloud and fog which may affect the detection of open water via the MOD29 process. This effect is observable in several instances, as seen in figure 14. On calm days, the fog will persist over the open water, resulting in cloud readings as shown in the figure. This is a case of lost observations but correct results. On windy days, the fog will drift over the surrounding ice. The concern with low, warm clouds over ice is that the MOD29 process may mis-interpret these signals as open water, however comparison with the Landsat data indicates that this does not appear to be a common problem. In the cases observed with Landsat, the cloud is correctly classified, although visual interpretation of the Landsat imagery would likely allow the inference of open water.

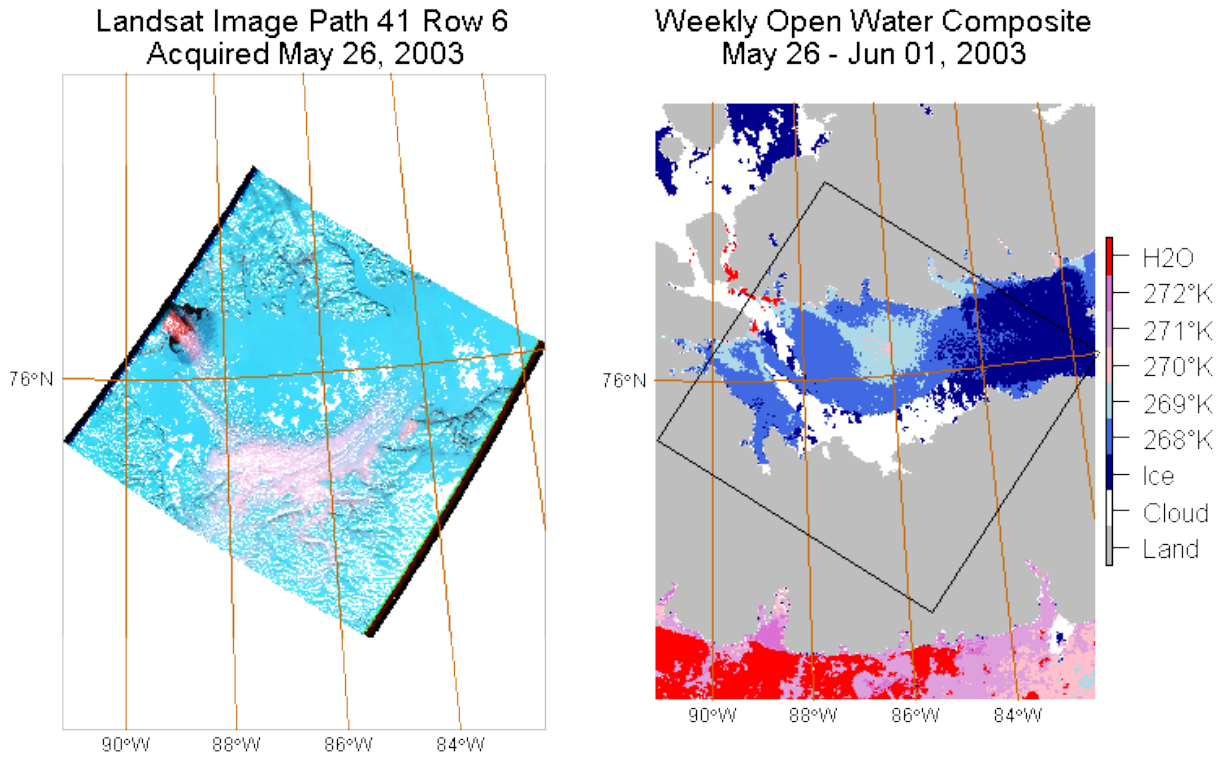

Figure 14: Persistent Cloud Cover: The dark open water evident at the western edge of this Landsat image is the Hell Gate Polynya, the red and white feature obscuring it is low cloud, which is echoed in the Weekly Open Water Composite result.

Proximity to Land

A relatively course land mask is applied to the MOD29/MYD29 grids, which likely results in missing some polynya features that occur in close proximity to the shore line. One obvious case is Bellot Strait, illustrated in figure 15. This effect is also evident at Hecla and Fury Straits.

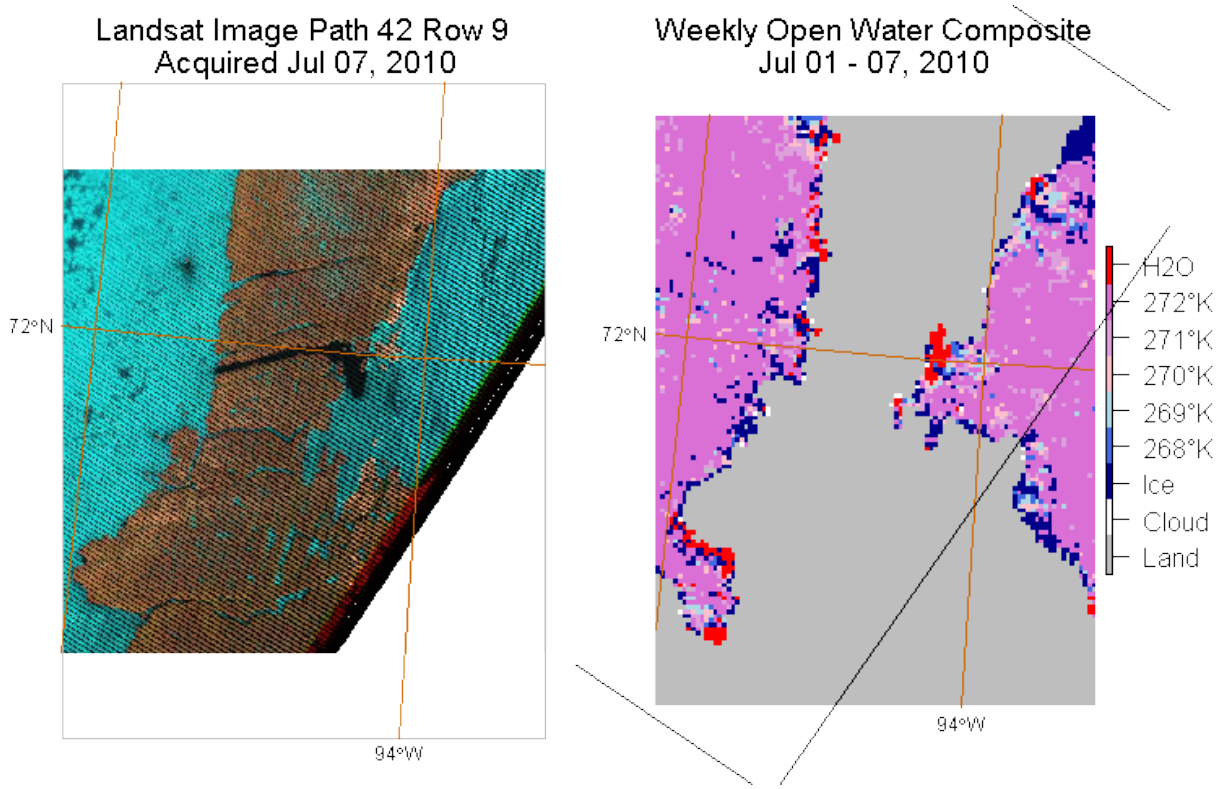

Figure 15: Landsat Comparison - Bellot Strait 2010: Bellot Strait is the narrow channel visible at the center of the Landsat image. Due to the coarse landmask applied to the MODIS sea ice product, this feature is not present in the MOD29 data.

Errors in MOD29/MYD29 Results

The primary limitation on the detection results obtained with the MOD29/MYD29 data is the presence of cloud, an effect which has been addressed by reducing the temporal resolution of the analysis to 7 days. In spite of this, there remain several locations which exhibit perennial cloud cover which may be indicative of the presence of open water. In order to validate the classified results, several hundred Landsat images were reviewed alongside the classification for the corresponding date. Based on this review, errors in the quality of the MOD29/MYD29 can be summarized as follows:

- Detection errors appear to be primarily type I errors, or false positives, where open water is reported for a location that is in fact ice covered. This effect seems to be related to periods of melting, when water pools on the ice surface, which implies that the sensor is actually observing water, but the interpretation of open ocean is incorrect. The impact of this type of error on the results is mainly restricted to the late spring and summer time months.

- Type II errors, or false negatives, where open water exists but is recorded as ice, seem to be less common, although a more thorough validation process would help to quantify where these problem might occur. Consideration of this type of error is certainly affected by the resolution of the source data. There area likely many cases where small openings in the ice with an extent of less than one square kilometer will

be reported as fully ice covered. Due to the integrating nature of the sensor, these situations would likely be reported as warmer ice.

In the above analysis, errors where either water or ice are reported as cloud are not considered since the processing and subsequent analysis treat cloud observations as missing data.

Analysis

Spatial Distribution of Polynya Features

Comparing the calculated EPO results with a well known map of recurring polynya features, there is a strong correspondence between the EPO results from the week of April 21-27 as shown in the following figures.

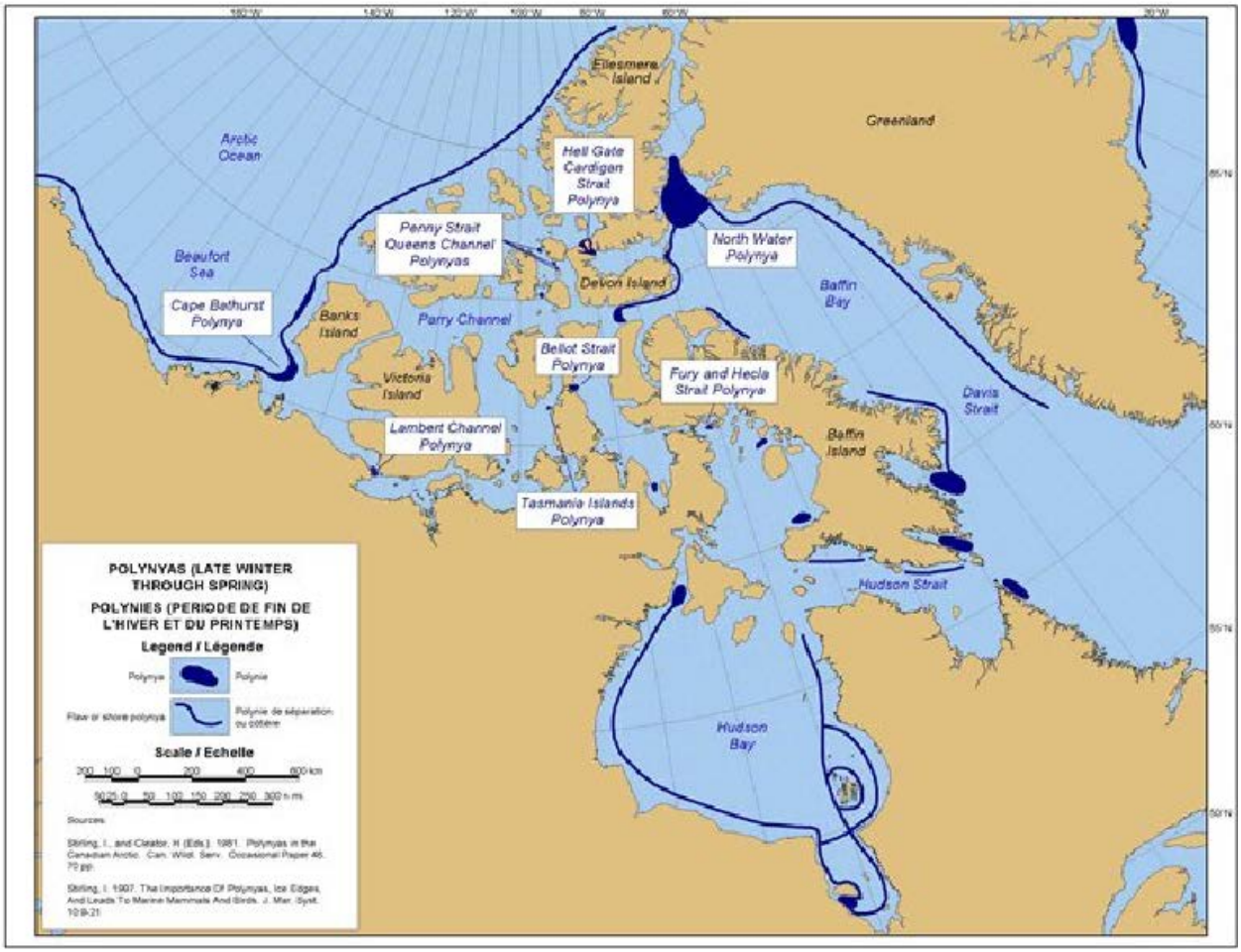

Figure 16: Polynya Locations Canadian Coast Guard: This map is taken from the publication Ice Navigation in Canadian Waters, showing locations of polynyas in mid-spring. Locations are taken from historical ice charts.

In the EPO result from mid April, most of the recurring polynya locations are represented with the exception of the Lambert Channel polynya, which appears to open sometime in May. Many other, smaller leads and polynyas are also evident in the data, mainly scattered throughout Baffin, Hudson and Committee Bays.

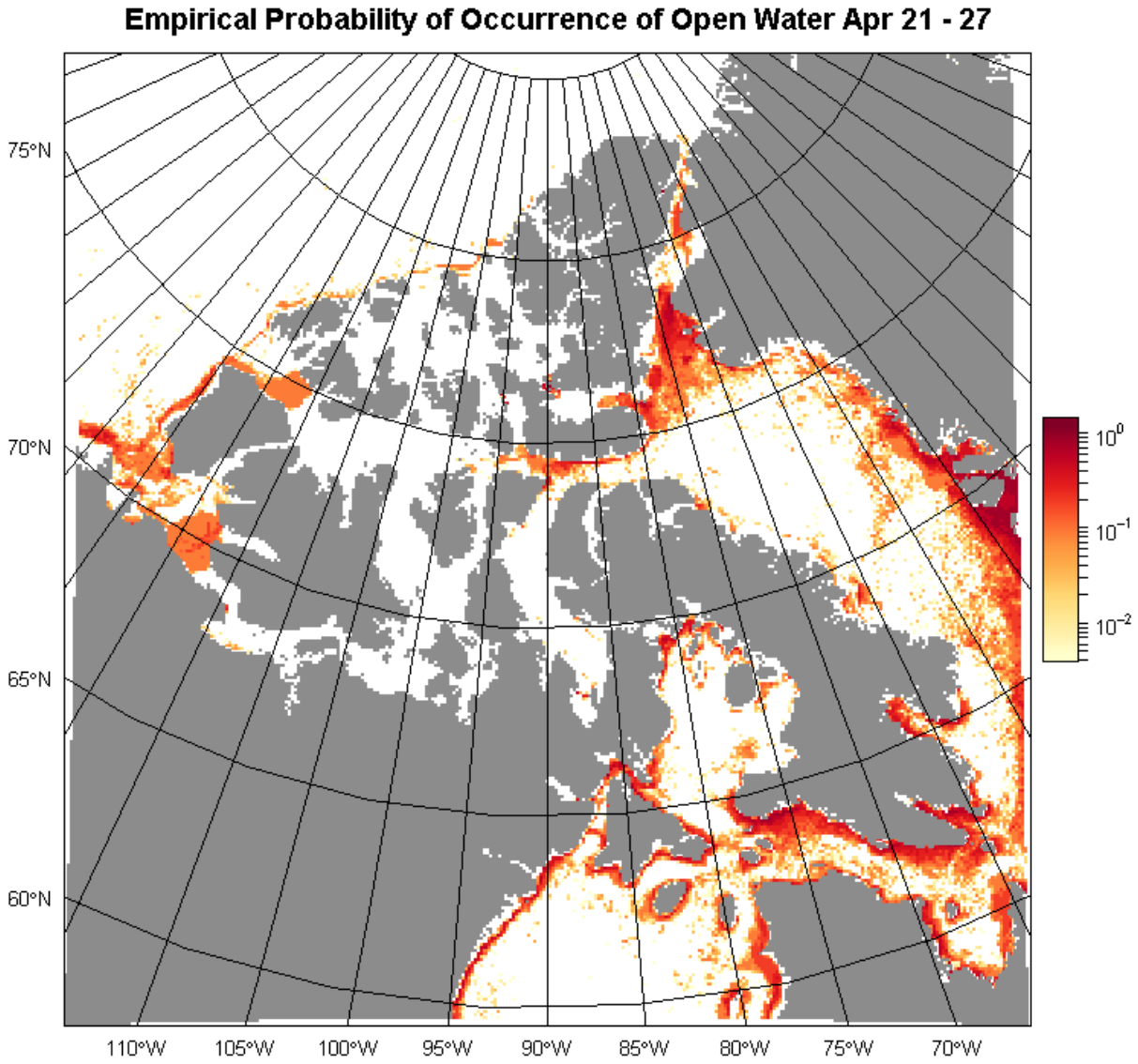

Figure 17: Mid Spring EPO April 21-27 - A logarithmic scale has been applied to this 4 km EPO grid from mid-April in order to accentuate the locations with higher probability of open water. This time period most closely conforms to the locations indicated in the CCG map in the previous figure.

Trends observed in the results

Working from the weekly open water composite grids, we can calculate the area for any of the available classes and compare throughout the project time frame. Figure 18 shows the variation for the open water and cloud classes for the entire project area.

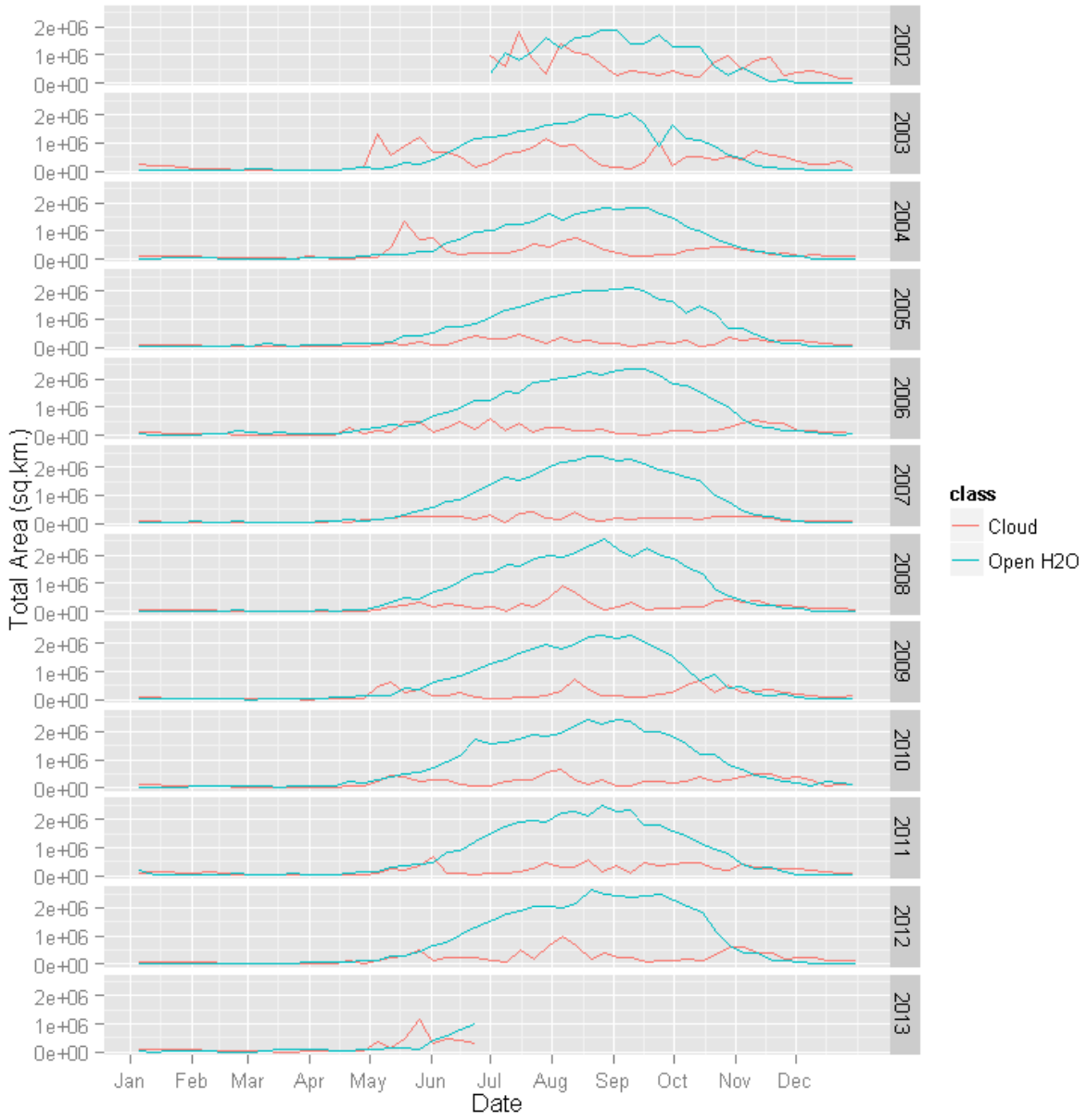

Figure 18: Cloud and Open Water Frequency Variation: These graphs show the amount of open water and cloud detected throughout each year from 2002 to 2013. Plotting the cloud frequency indicates the limitations of the data and aggregation methods - higher cloud values indicate greater uncertainty in the open water result. Seasonal variations in open water area is evident between summer and winter. The polynya signal is most prominent in the March-May period.

It is useful to review the variation of the cloud frequency, as the rather high values through 2002 and 2003 are indicative of the lack of data which could be used to reduce the cloud signature. Also, there are several epochs at which the cloud and water lines appear to spike in opposite directions, suggesting that the lower open water areas reported at those points may be obscured by cloud. This appears to occur in late September 2003, for example.

With respect to yearly variations in the open water areas, the most striking effect appears to be the deflection in the curves at the beginning of June in 2006, 2012, and to a lesser extent 2003.

Open Water Fraction

Although there are some periods where in spite of aggregation, the amount of cloud is equal to or higher than the detected open water, inspection of the Weekly Open Water Composite results suggests that the cloud occurrence is randomly positioned and should not strongly influence the interpretation. For defined geographic areas, we can eliminate the cloud from interpretation by calculating the open water fraction, as:

$$OpenWaterFraction = \frac{\sum_{H_2O}}{\sum_{H_2O+Ice}}$$

Figure 19 illustrates the overall variation of this statistic through the project period (2002-2013).

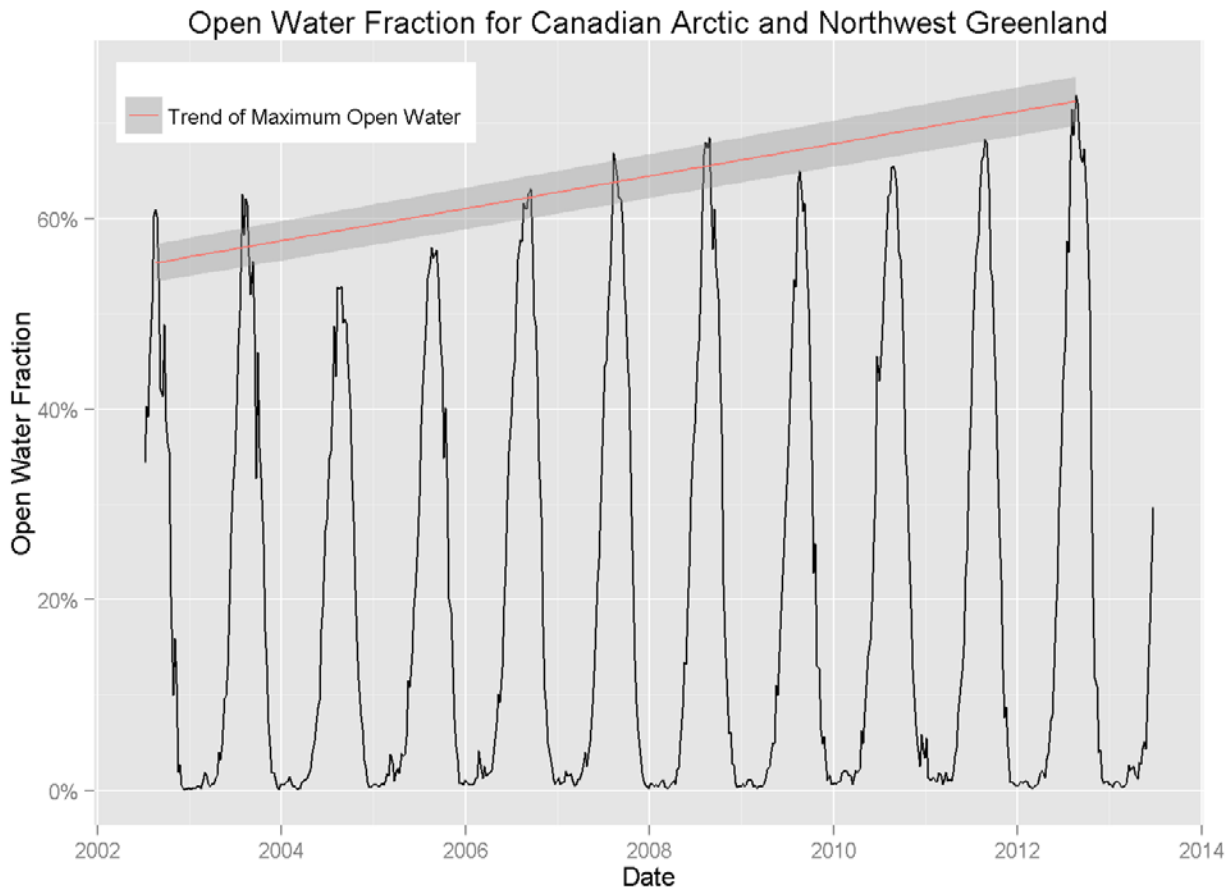

Figure 19: Open Water Fraction Variation: This graph shows the fraction of open water detected throughout the project timeframe for the overall area.

This chart clearly reflects the annual variation in open water in the region, and the general trend towards larger areas of open water during summer illustrated by the red line fit to

the maximum values. The largest open water fraction was attained in the summer of 2012. Comparing this result on a year by year basis, as shown in figure 20 illustrates the large variation during the summer months.

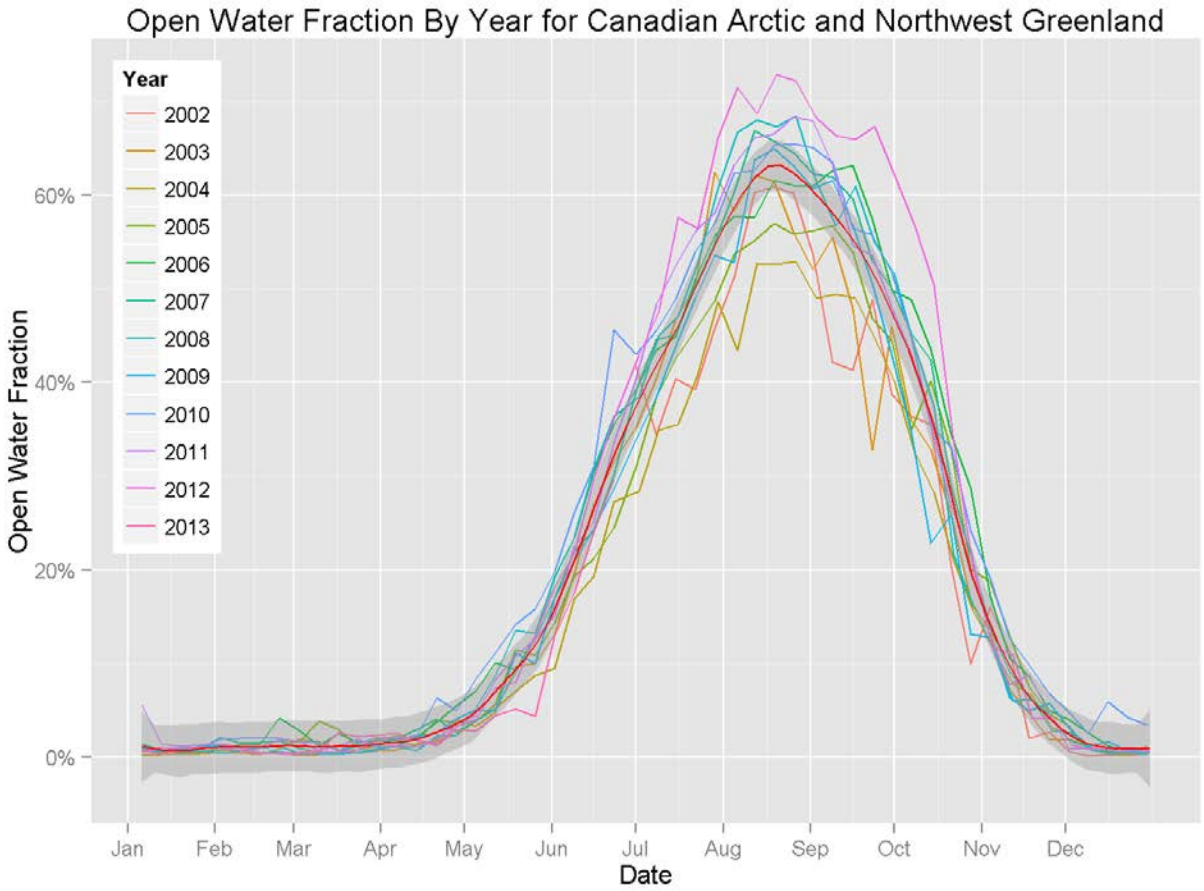

Figure 20: Open Water Fraction Variation By Year: This graph compares the open water fraction for the entire area on a year by year basis. The majority of the variation is evident in the summer. Note the curve shown in red illustrates the mean over the 11 year study period, with a 99% confidence level indicated in gray.

While many polynas persist throughout the year, they will have a thin ice cover during the winter months and may be surrounded by open water in the summer and fall. The polynya signal is therefore most prominent in the spring months of March through May, so we need to focus on that time period. We can compare the open water fractions during the spring period, as shown in figure 21 to get a more detailed view of the year over year variation.

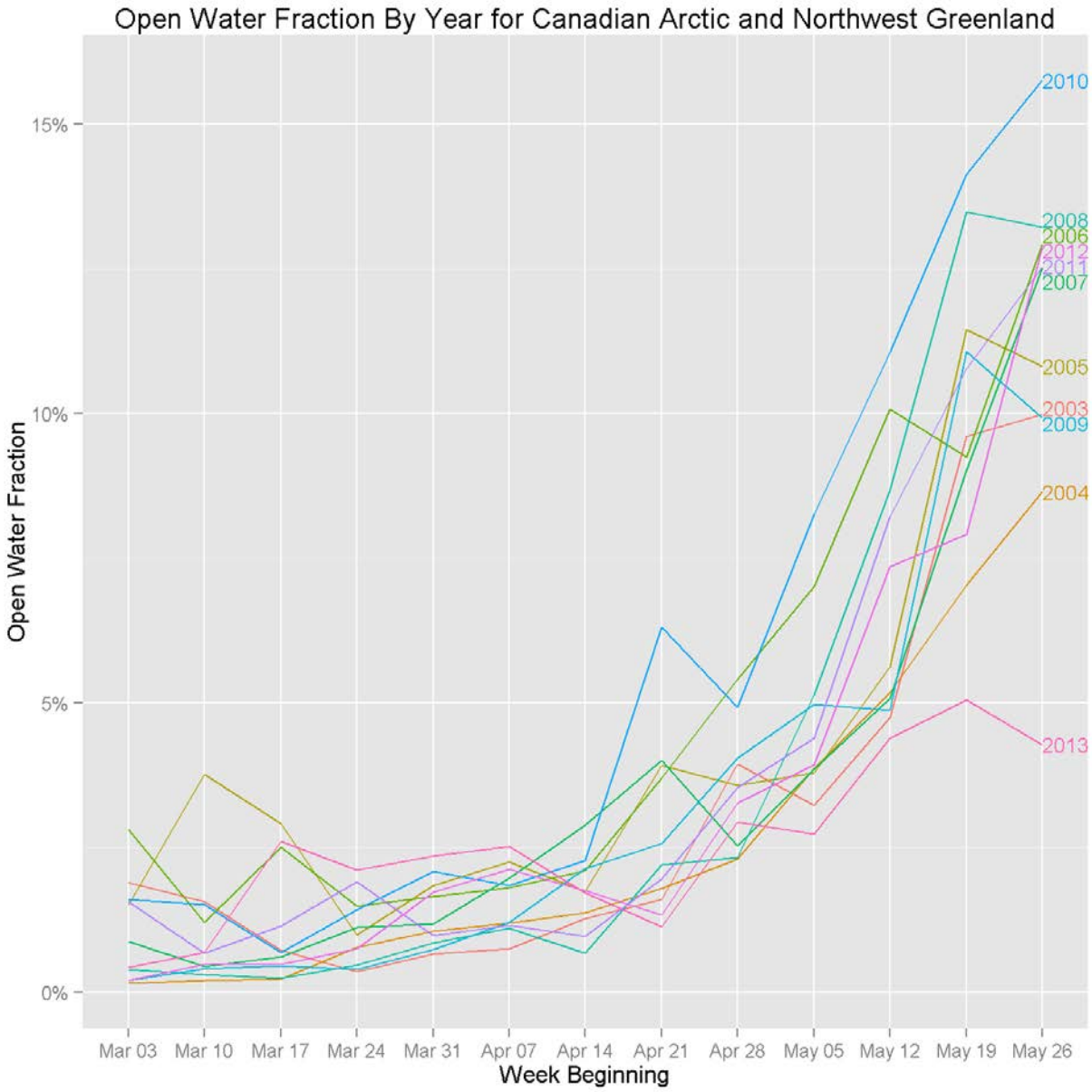

Figure 21: Open Water Fraction Variation For Spring Period: These graphs show the amount of open water detected throughout each of the eleven years from 2003 to 2013 during the key March to May time period.

Interpreting the above graphic, we can see that the years 2005 and 2006 exhibit higher open water areas in March than other years. By the end of May, large areas of open water are observed and the polynya signal begins to disappear, particularly in 2010, with the years 2003, 2004, 2009 and 2013 showing lower than average amounts. At this scale, the polynya signal appears in the range of 2% to 5% of the area.

Spatial Variance of Empirical Probability of Occurrence

Working from the empirical probability of occurrence grids, we can calculate a spatial view of variance from the mean for each epoch, or point in time. The following graphic illustrates where, and in which years, the probability of occurrence of open water is higher and lower than the mean taken over all years, for a single week.

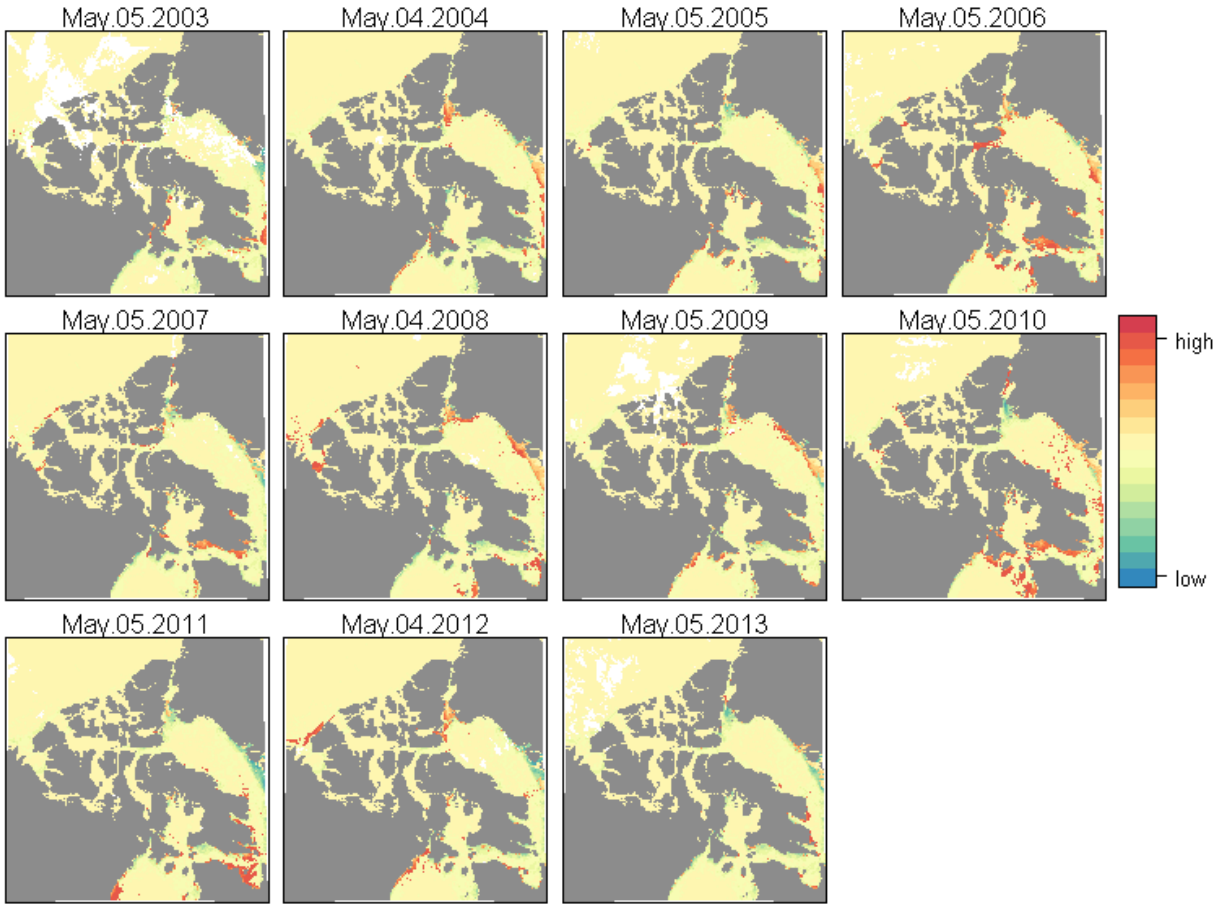

Figure 22: EPO Deviation From The Mean: These diagrams show the spatial distribution of the difference between the yearly EPO value and the EPO value computed for all years, for the week beginning May 5. Areas shown with high variation (red) indicate there was more open water in that year than was detected over all years, blue indicates less open water.

Based on this analysis, we can see that the years 2004, 2006, 2008, 2009, and 2012 represented higher than average occurrences of open water in the mid-spring time frame.

For example, in the week shown above, it appears that the Cape Bathurst polynya had much more open water than normal in early May 2012. Similarly, the Lambert Channel polynya saw it's maximal extent in 2008.
A complete set of these variance maps may be reviewed in Appendix E.

Spring Comparison

Another approach to compare yearly variation is to compare the area of open water detected in a specific week over the eleven year period. The polynya signal is most easily detectable in the spring, when the polynyas are less likely to have a cover of thin ice and melting has increased their extents but before general breakup has begun. The graphs in figure 23 illustrate how the fraction of open water varies by year, comparing a period of four weeks beginning April 28.

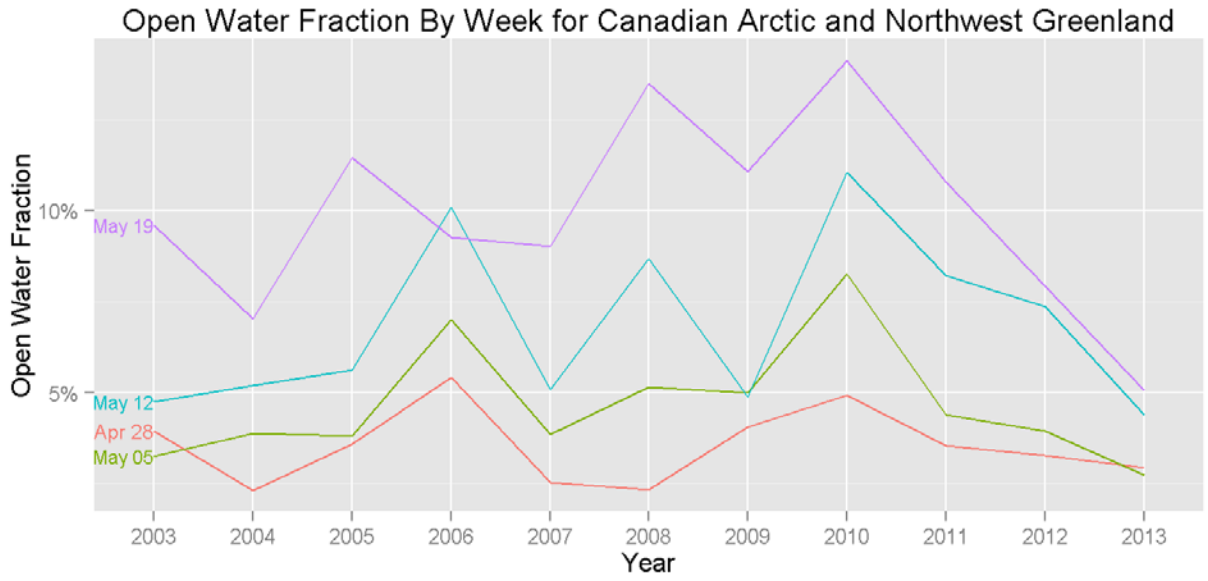

Figure 23: Spring Open Water Fraction Variation By Year

Clearly, there is considerable variation between years as well as week to week within a particular year. If we take the week beginning May 05 as the key date, the years 2006 and 2010 show the highest occurrence of open water while 2003 and 2013 show the lowest. The mean open water fraction during this week is 4.7%. The following maps illustrate how this appears in the weekly open water composite data.

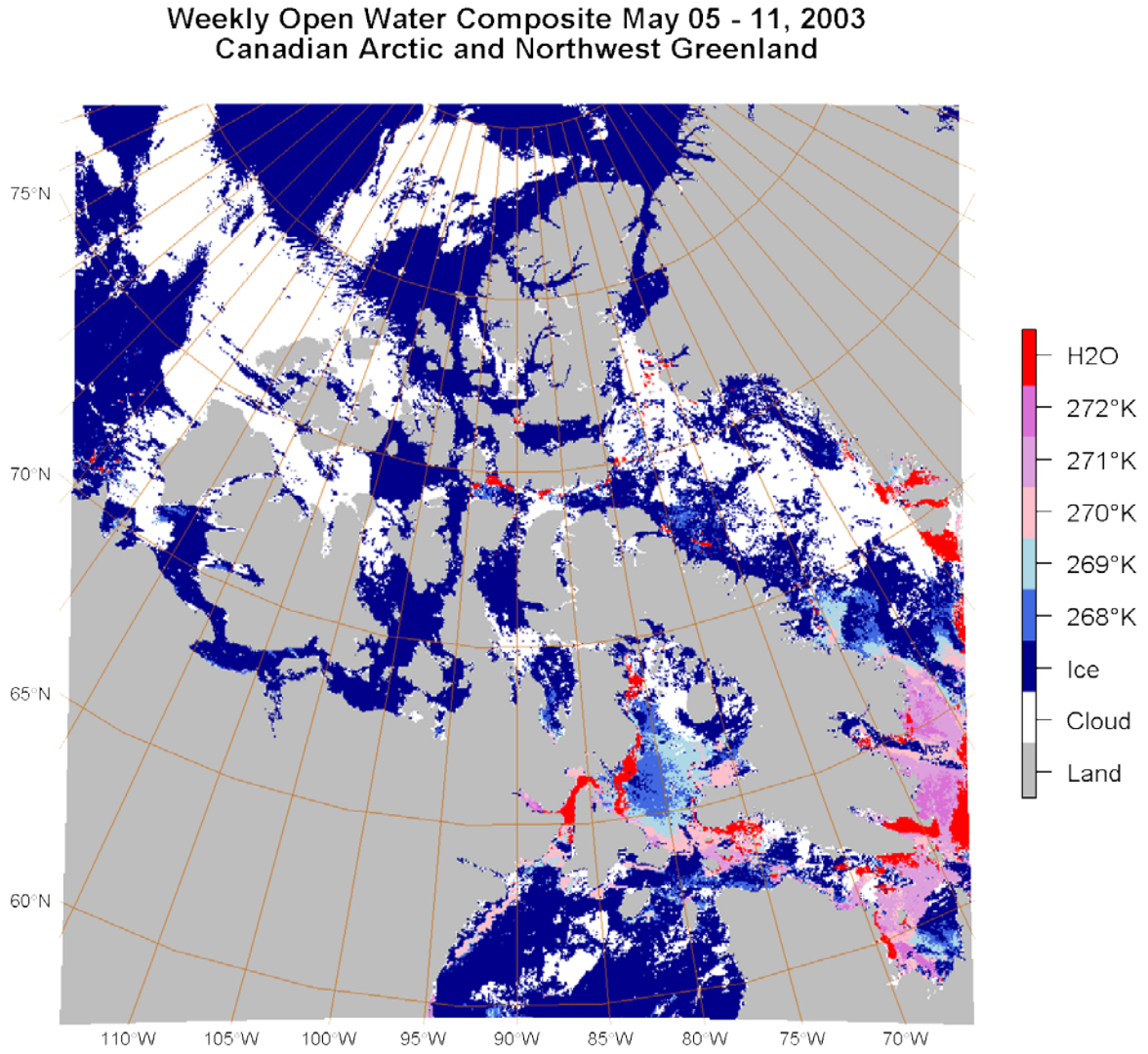

Figure 24: Weekly Open Water Composite - May 5, 2003: Open water represents 3.2% of the non-land area. Note the significant amounts of cloud (white). This is a result of the poor data availability from this time period which limited the effectiveness of temporal aggregation.

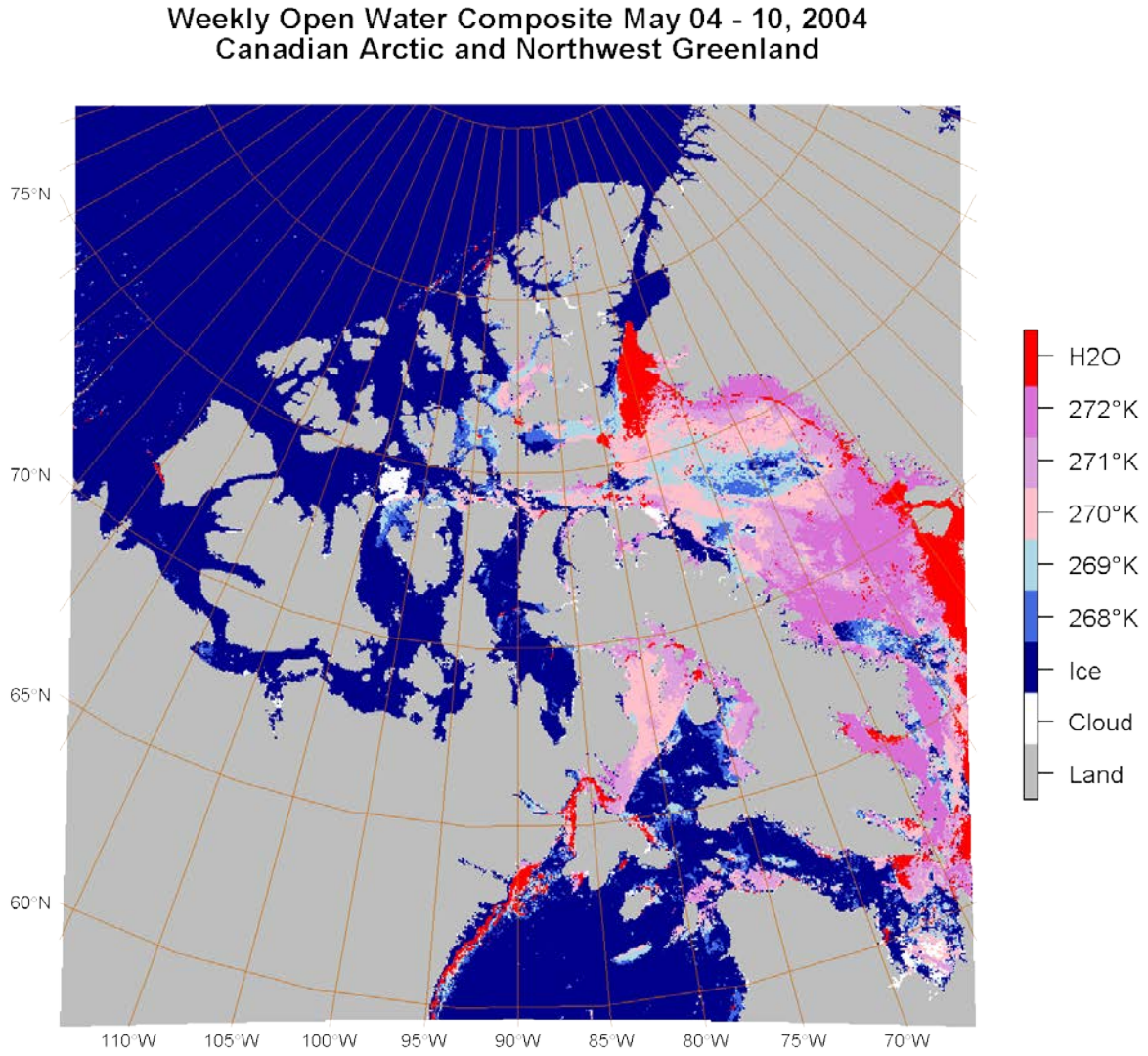

Figure 25: Weekly Open Water Composite - May 5, 2004: Open water represents 3.9% of the non-land area

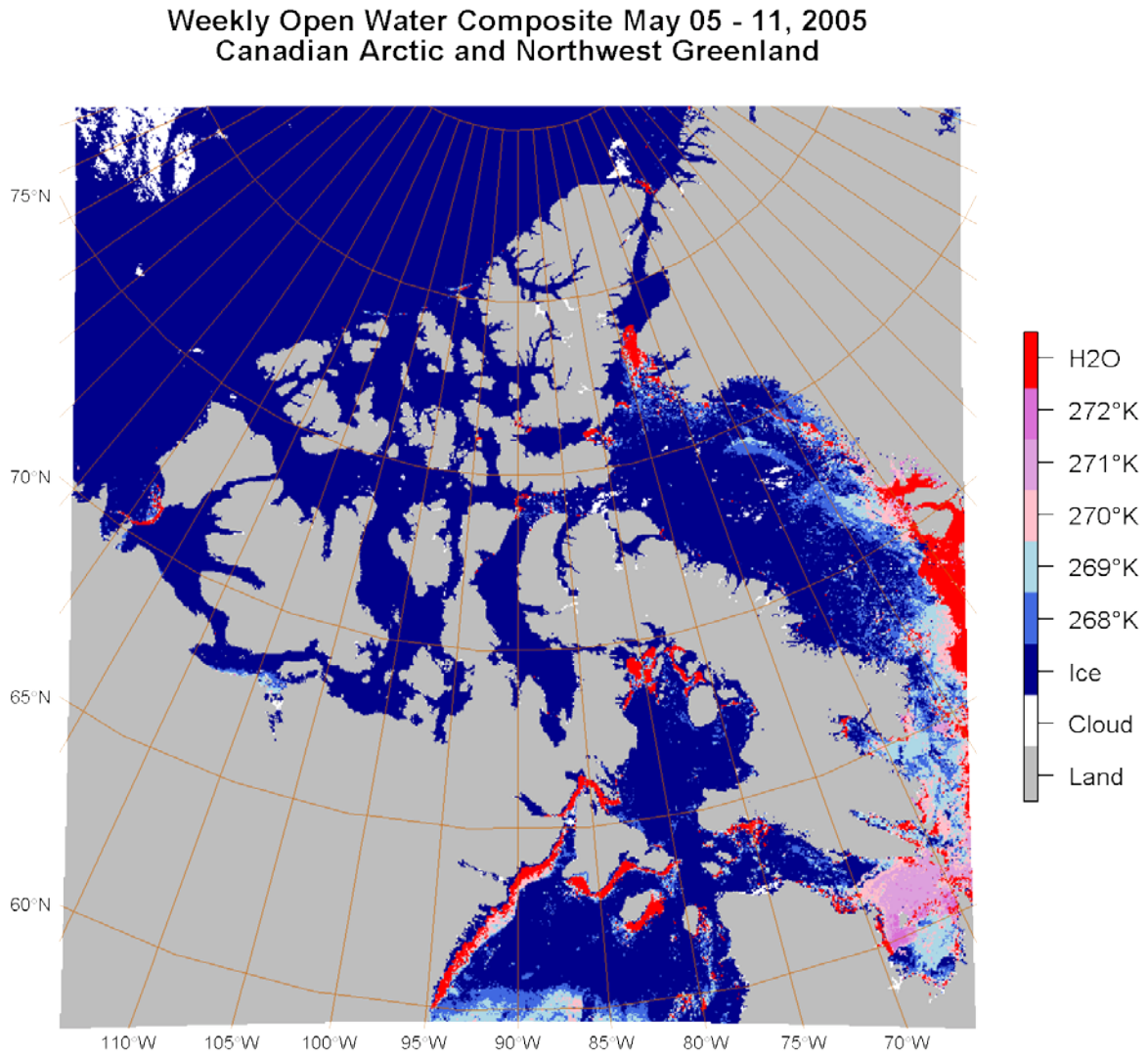

Figure 26: Weekly Open Water Composite - May 5, 2005: Open water represents 3.7% of the non-land area

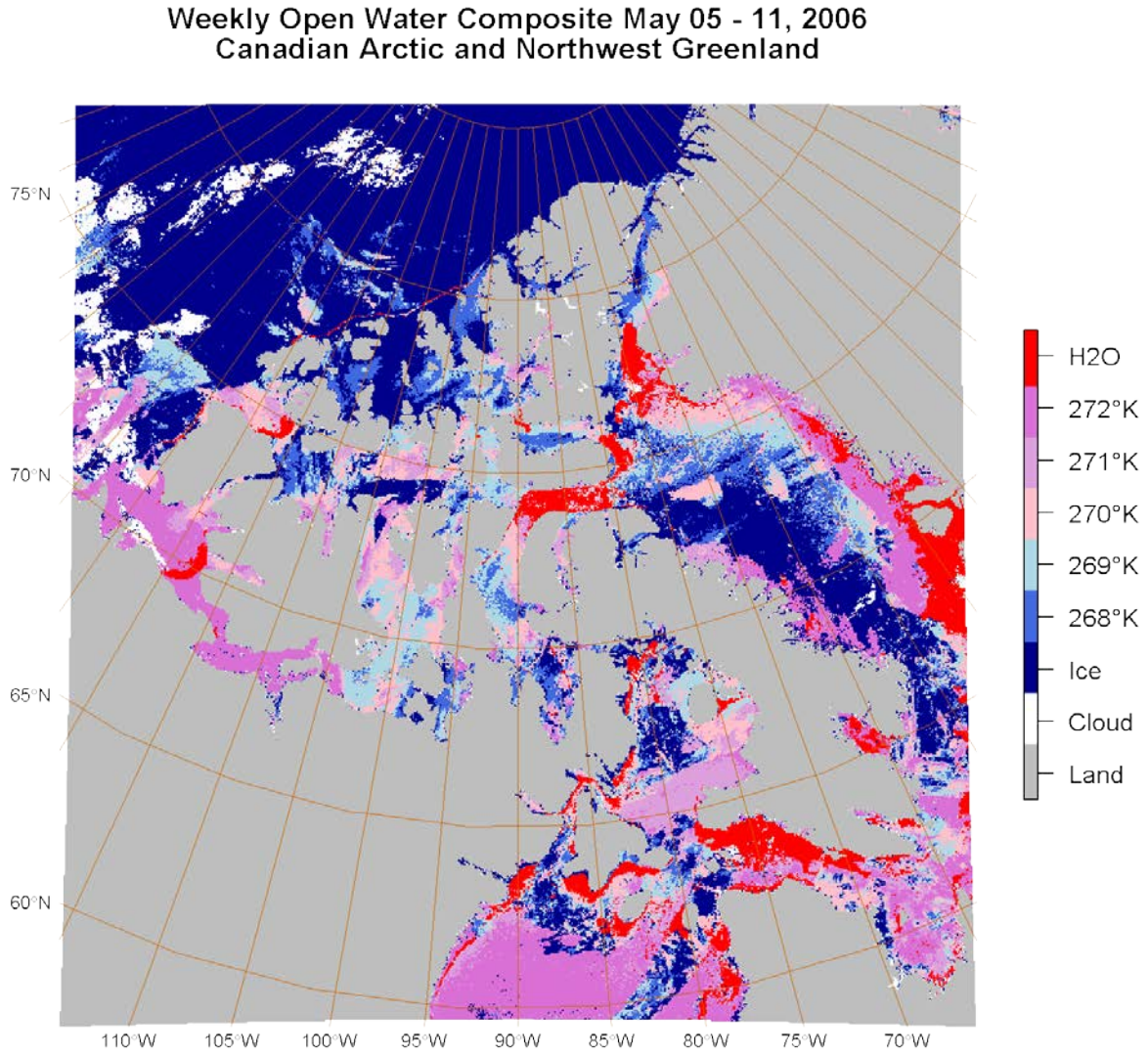

Figure 27: Weekly Open Water Composite - May 5, 2006: Open water represents 7% of the non-land area, the second highest value for this week.

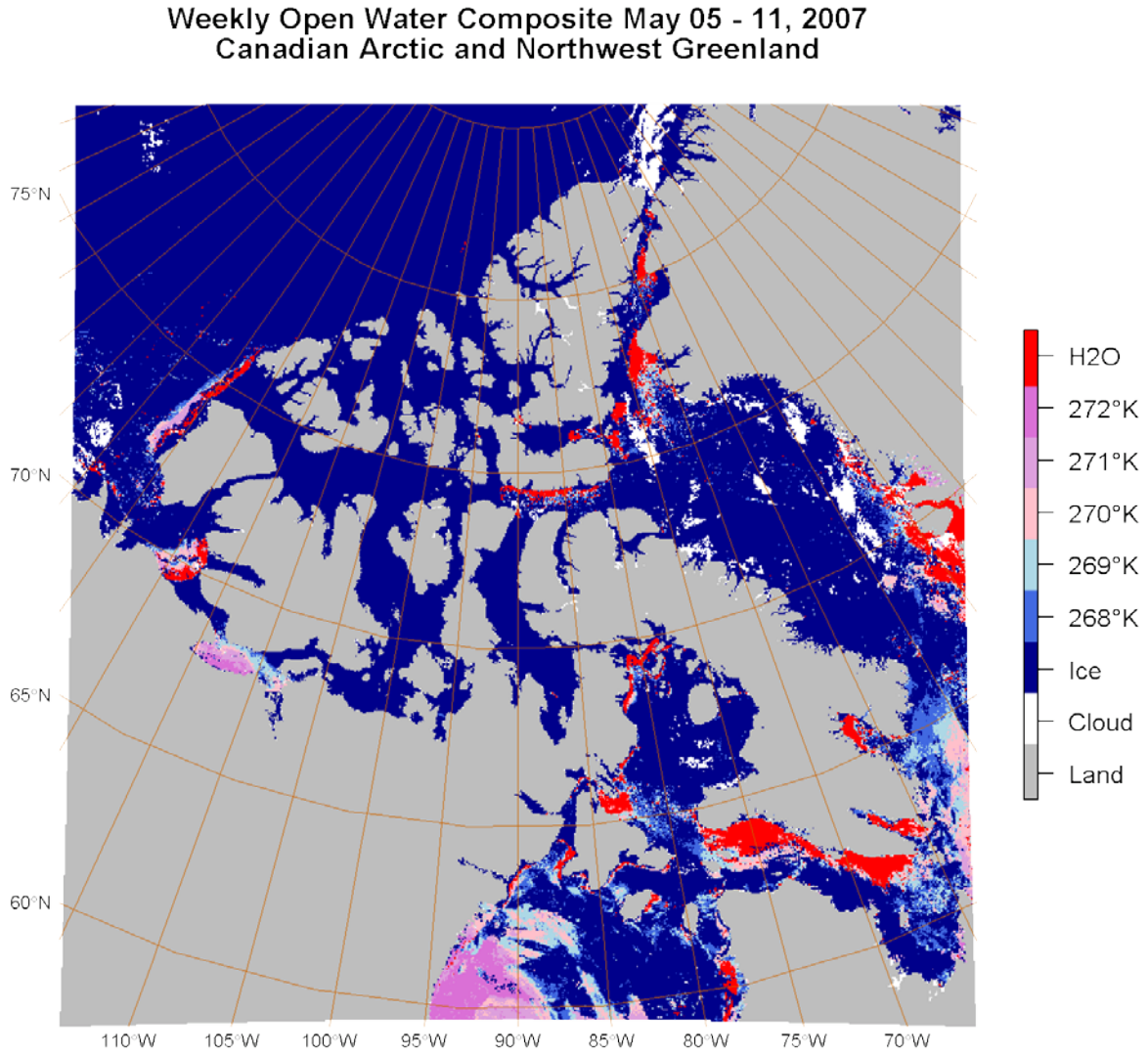

Figure 28: Weekly Open Water Composite - May 5, 2007: Open water represents 3.8% of the non-land area

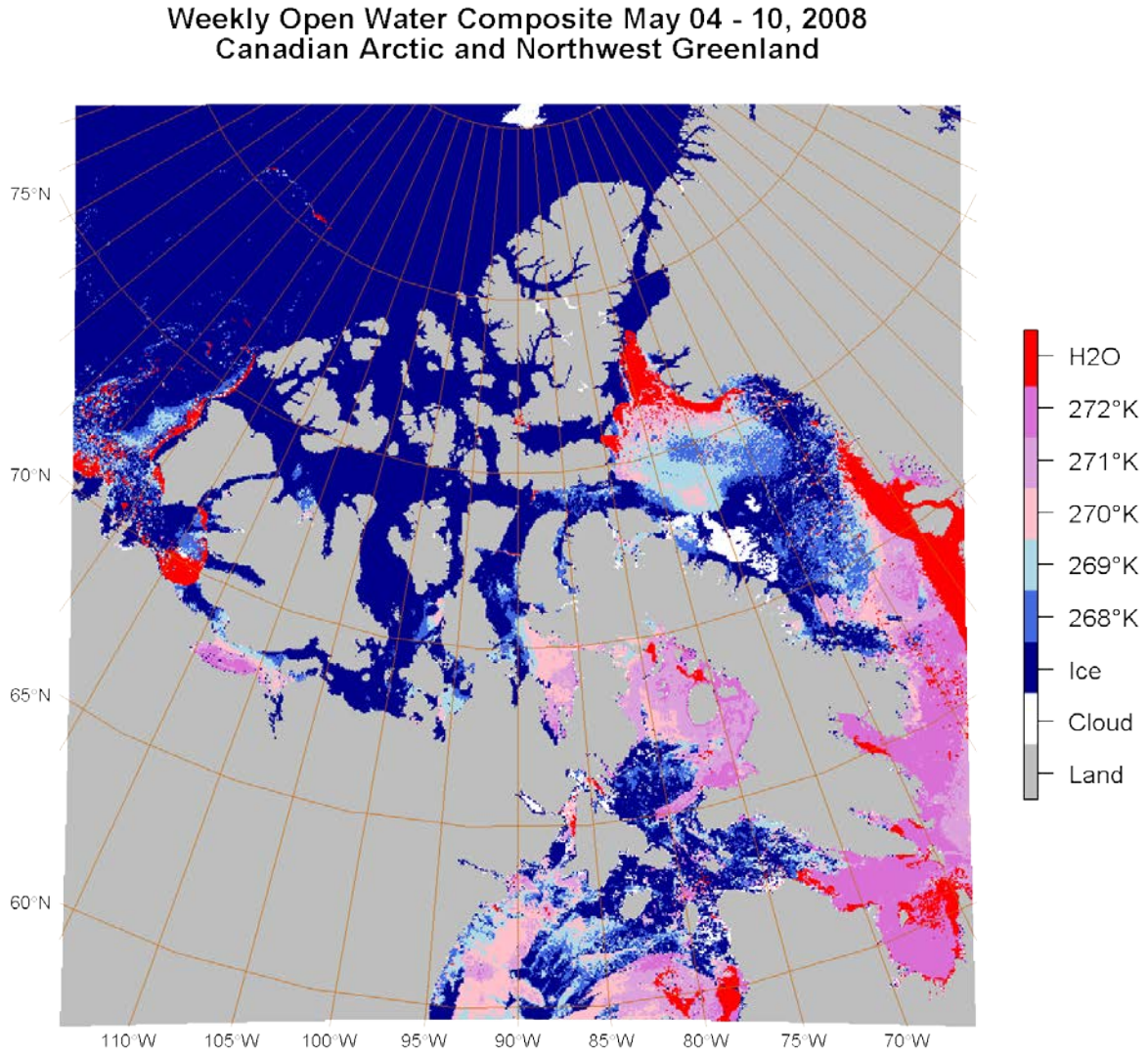

Figure 29: Weekly Open Water Composite - May 5, 2008: Open water represents 5.1% of the non-land area

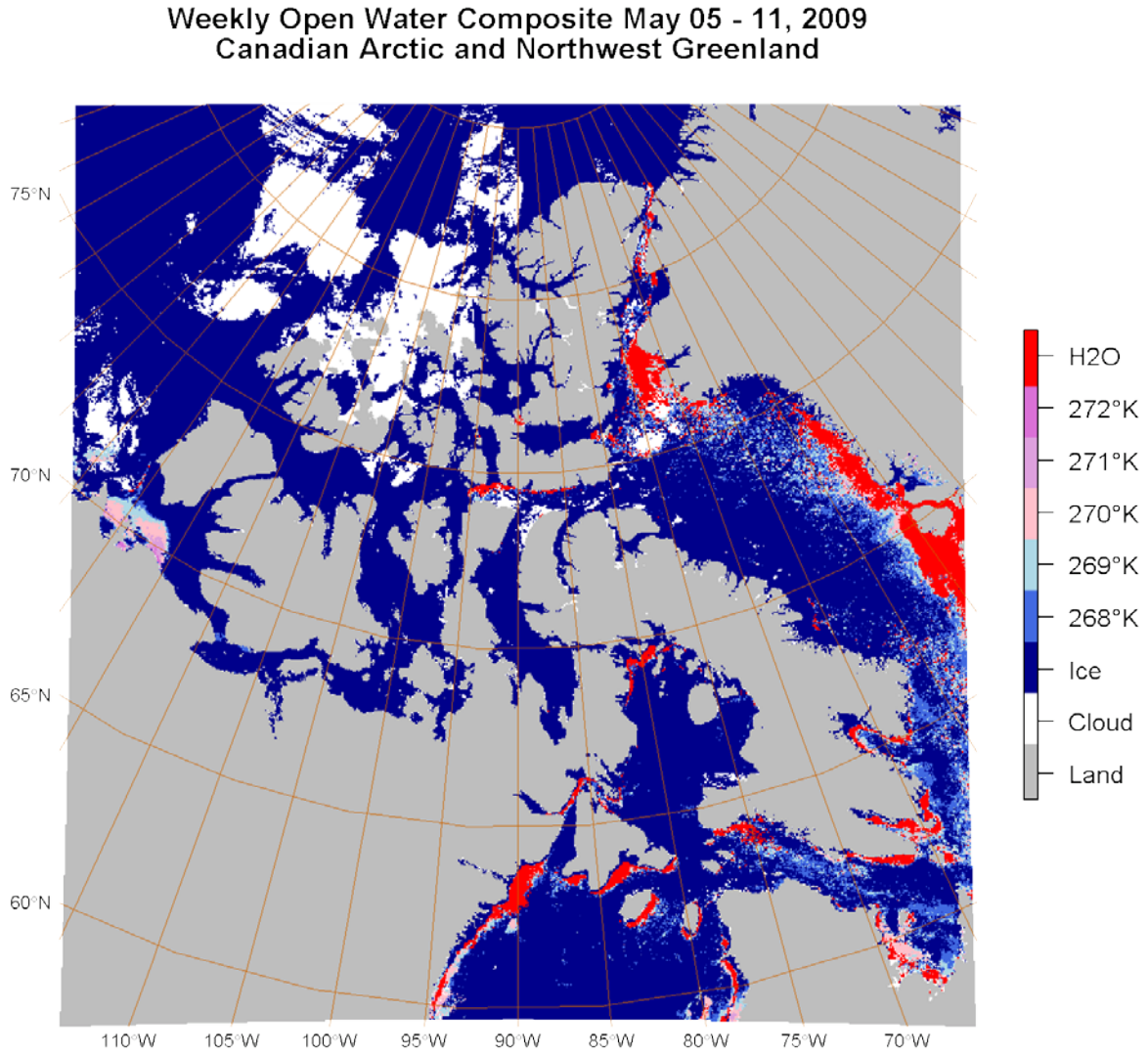

Figure 30: Weekly Open Water Composite - May 5, 2009: Open water represents 5% of the non-land area. Note significant amounts of cloud (white) are not located in areas where polynyas typically form.

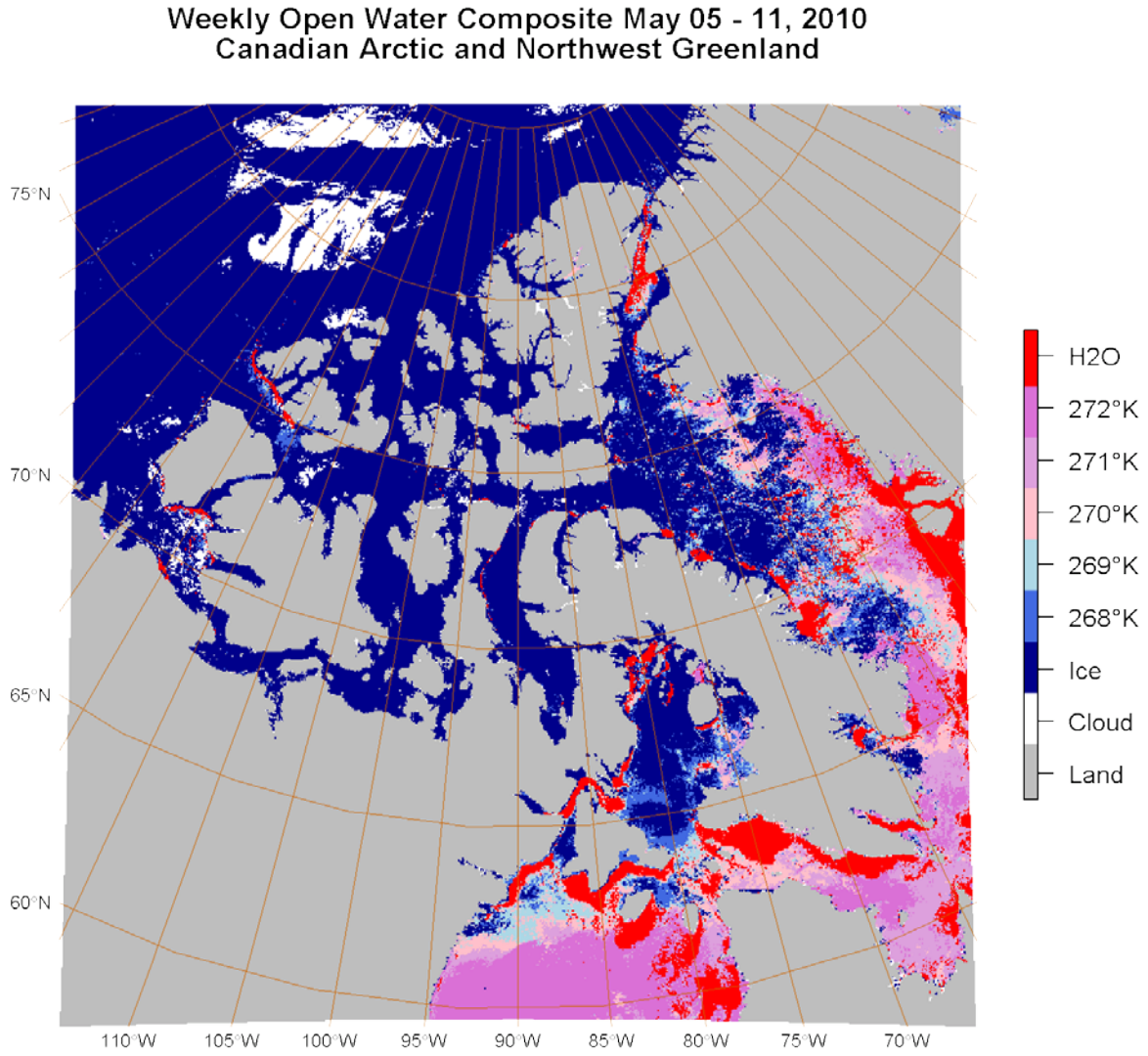

Figure 31: Weekly Open Water Composite - May 5, 2010: Open water represents 8.2% of the non-land area, the highest of the observed fractions for this week.

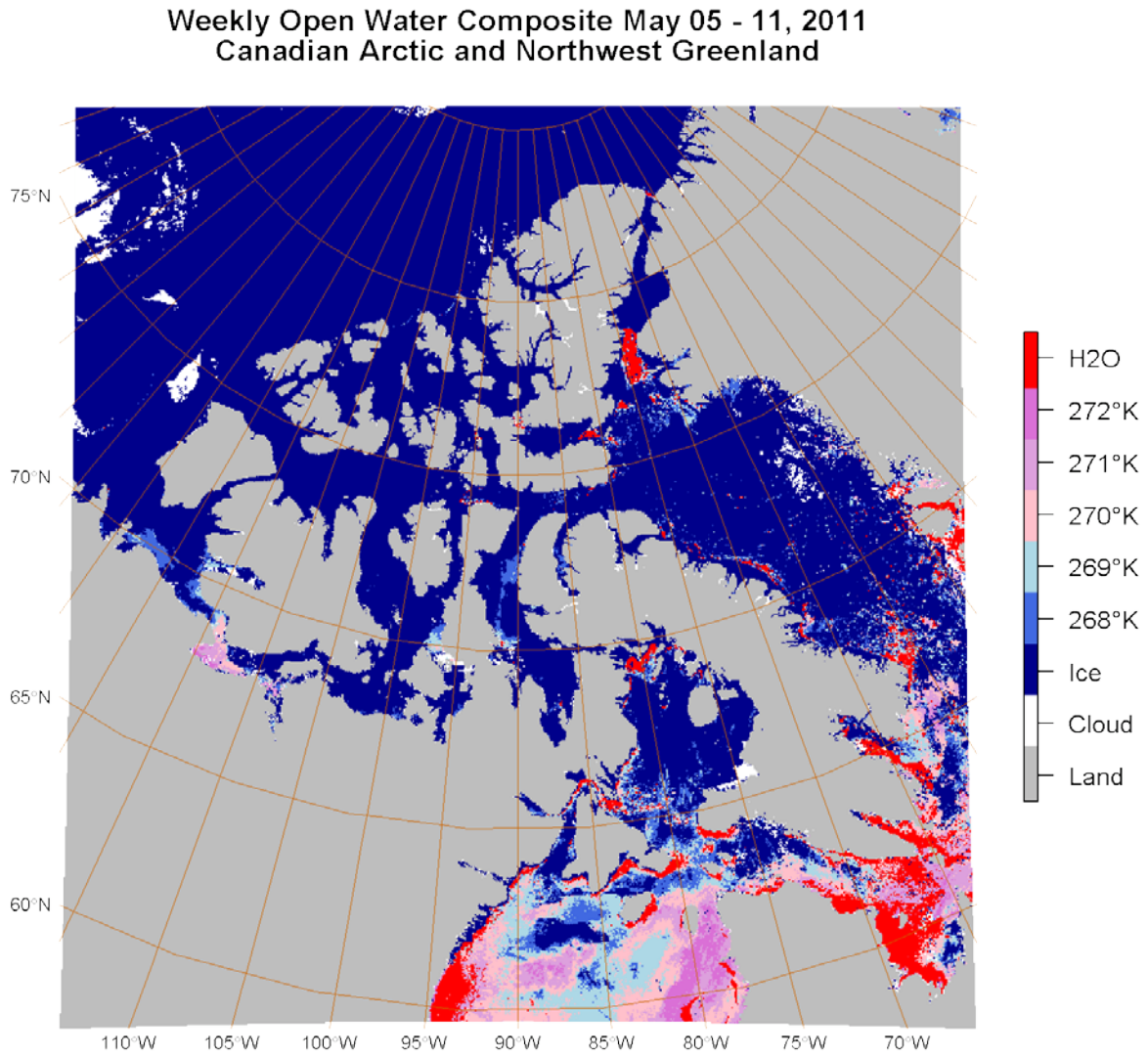

Figure 32: Weekly Open Water Composite - May 5, 2011: Open water represents 4.4% of the non-land area

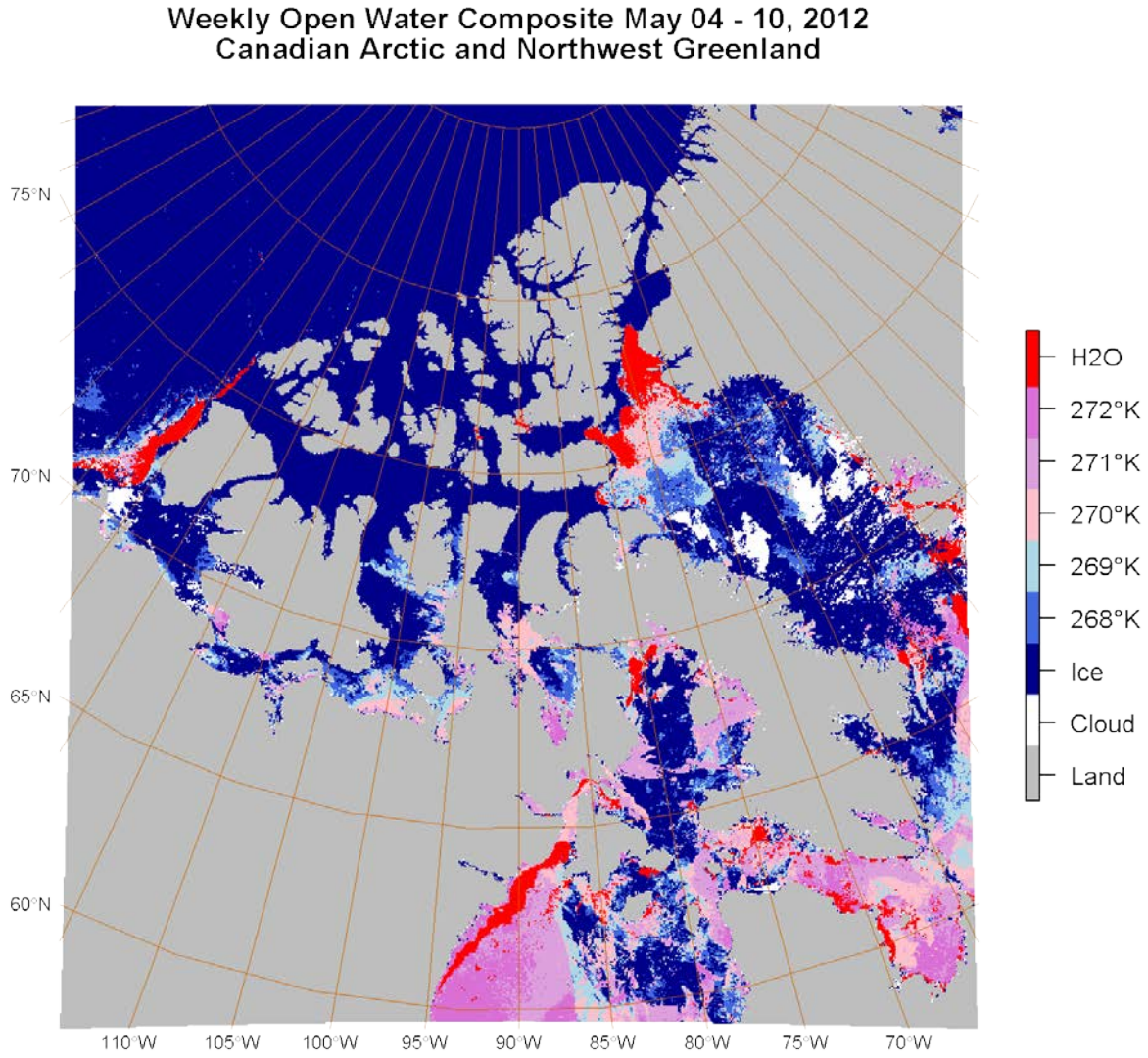

Figure 33: Weekly Open Water Composite - May 5, 2012: Open water represents 3.9% of the non-land area.

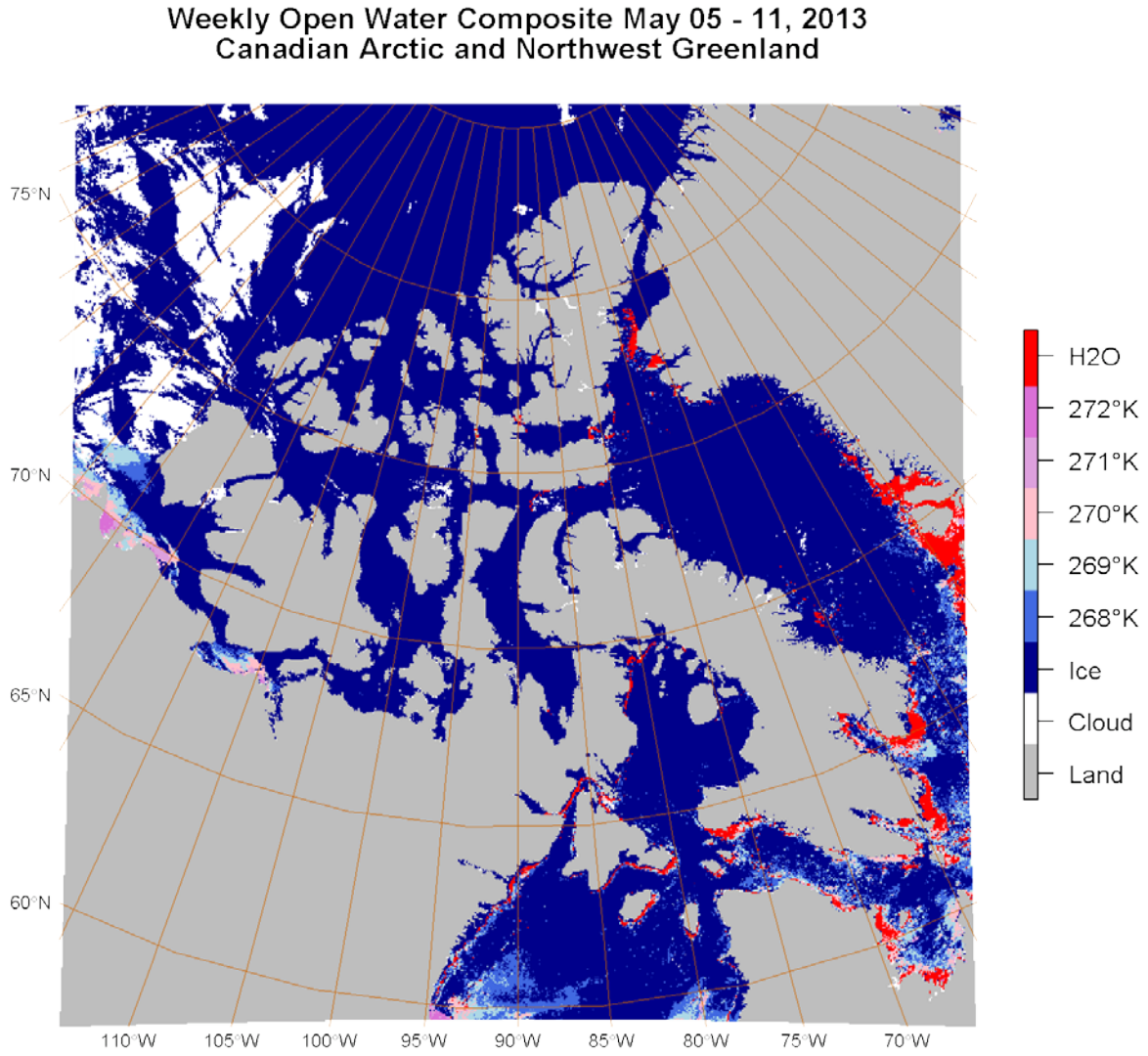

Figure 34: Weekly Open Water Composite - May 5, 2013: Open water represents 2.7% of the non-land area, the lowest of the observed fractions for this week.

Regional Analysis: Last Ice Area

The comparison of open water fraction between years discussed above is strongly influenced by the open water detected in Baffin and Hudson Bays. Restricting the analysis to an area with less open ocean may offer a clearer view of any trends in the data. Using the predicted last ice area over the northern part of the archipelago, we can recalculate the fraction of open water and display the variation in the same way, as shown in figure 35.

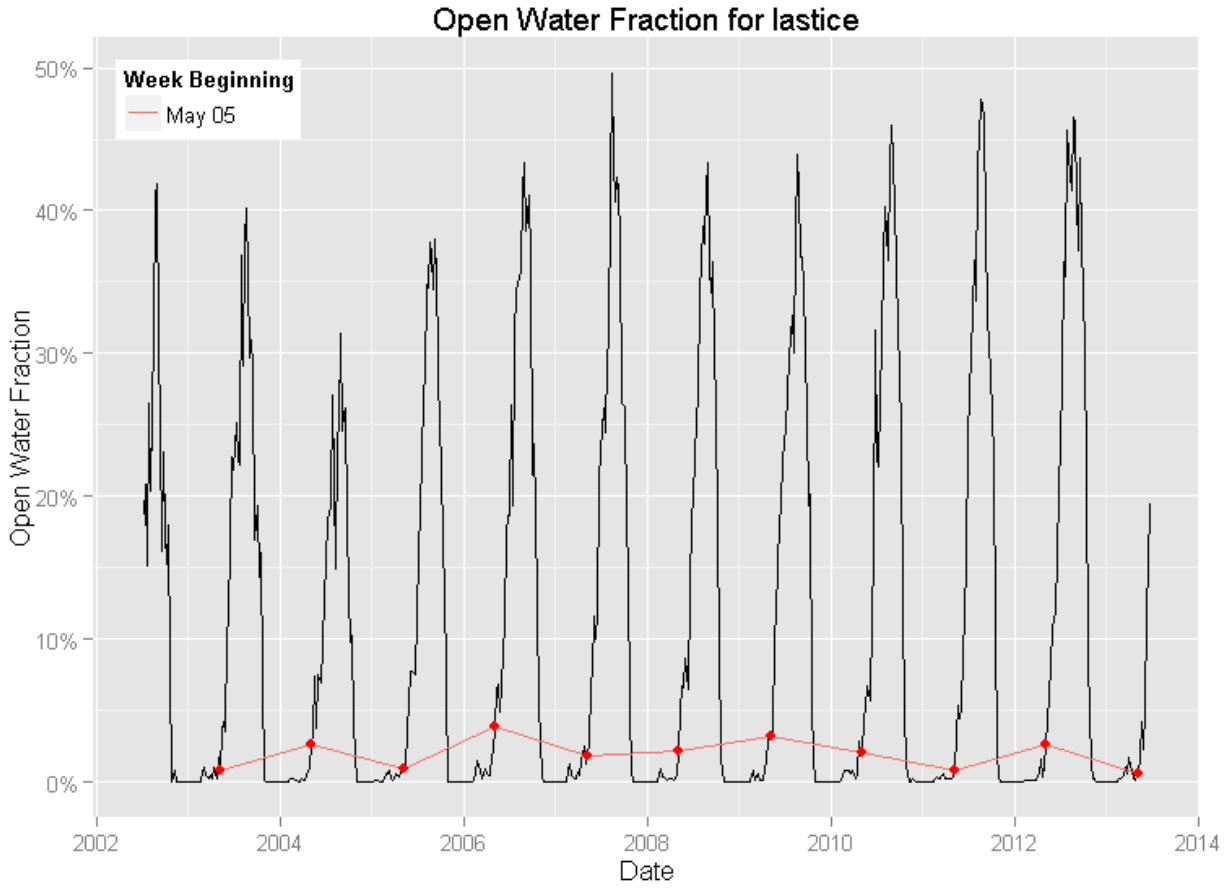

Figure 35: Spring Open Water Fraction Variation By Year - Last Ice Area

Once again, we see summer maximums of open water with distinct maxima in 2007 and 2011, and lowest extreme occurring in 2004. Using the week of May 05, highlighted in red, the highest fractions occur in 2006 and 2009, while the minima occur in 2003, 2005, 2011, and 2013. This suggests that the occurrence of large polynya features in the spring is not strongly correlated with maximum extents of open water at the peak of summer. The following figures show examples of these extremes and illustrate the extents of the analyzed area.

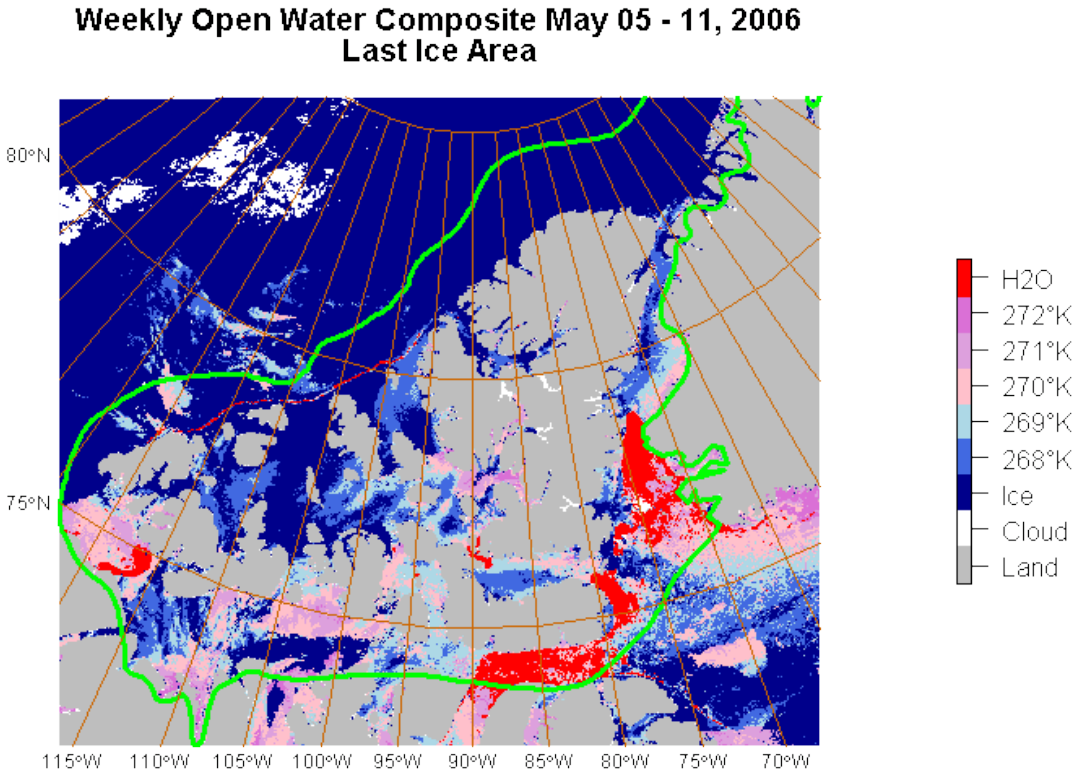

Figure 36: Weekly Open Water Composite - Last Ice Area - May 5, 2006: This represents the highest fraction of open water for this area at this time (3.8%). Note that the open water fraction is only calculated for water and ice areas within the green boundary.

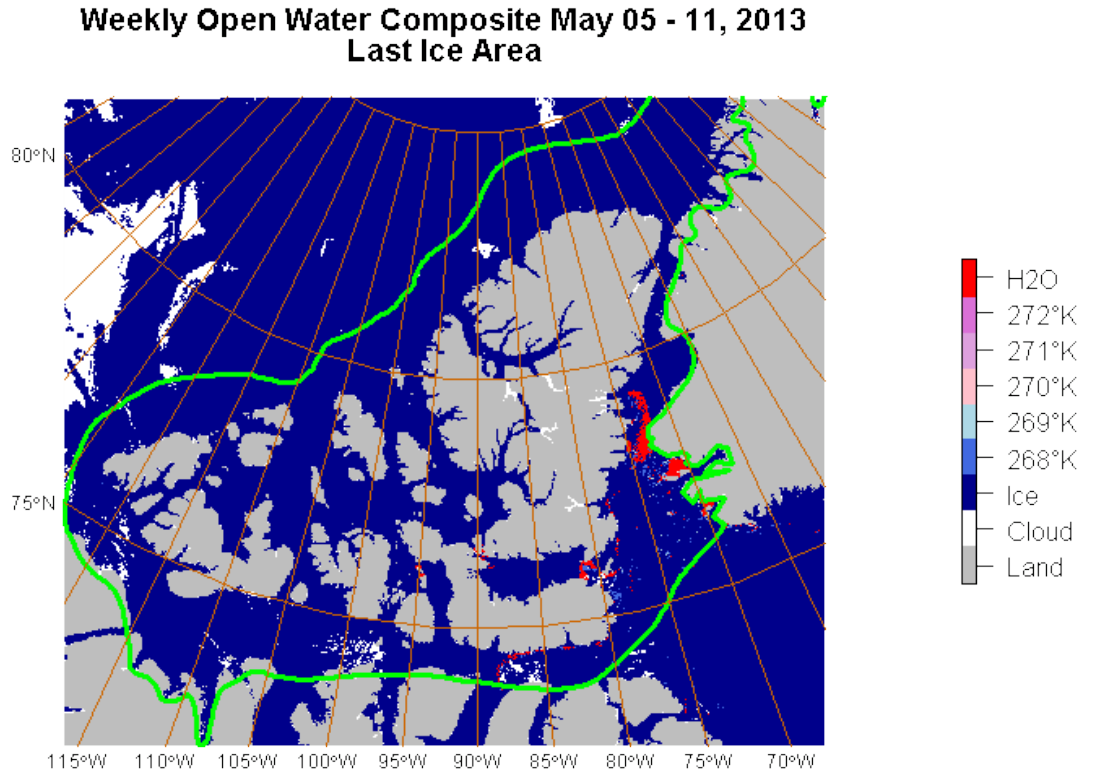

Figure 37: Weekly Open Water Composite - Last Ice Area - May 5, 2013: This represents the lowest amount of open water detected at this time (0.5%). Note that the open water fraction is only calculated for water and ice areas within the green boundary.

In this case, the difference in polynya size and frequency appears quite significant, and there is considerable evidence of warmer (presumably thinner) ice in the 2006 epoch.

Regional Analysis: Hell Gate - Cardigan Strait Polynya

Given the large area and time frame of this project, it is difficult to draw general conclusions regarding the occurrence and extent of polynyas that are applicable to all of the observed open water events. Focusing on a specific feature, such as the well known Hell Gate polynya in the vicinity of North Kent Island allows us to examine the results in some depth. The following series of figures show the classified result in this location compared with coincident Landsat images. The first from May 11, 2008 shows a well defined area of open water shown in red in the classified image, dark color in the Landsat scene, surrounded by sea ice with mostly warmer temperatures. Some thin ice, with surface temperatures in the range of 271°-273°K, is evident within the main bounds of the polynya.

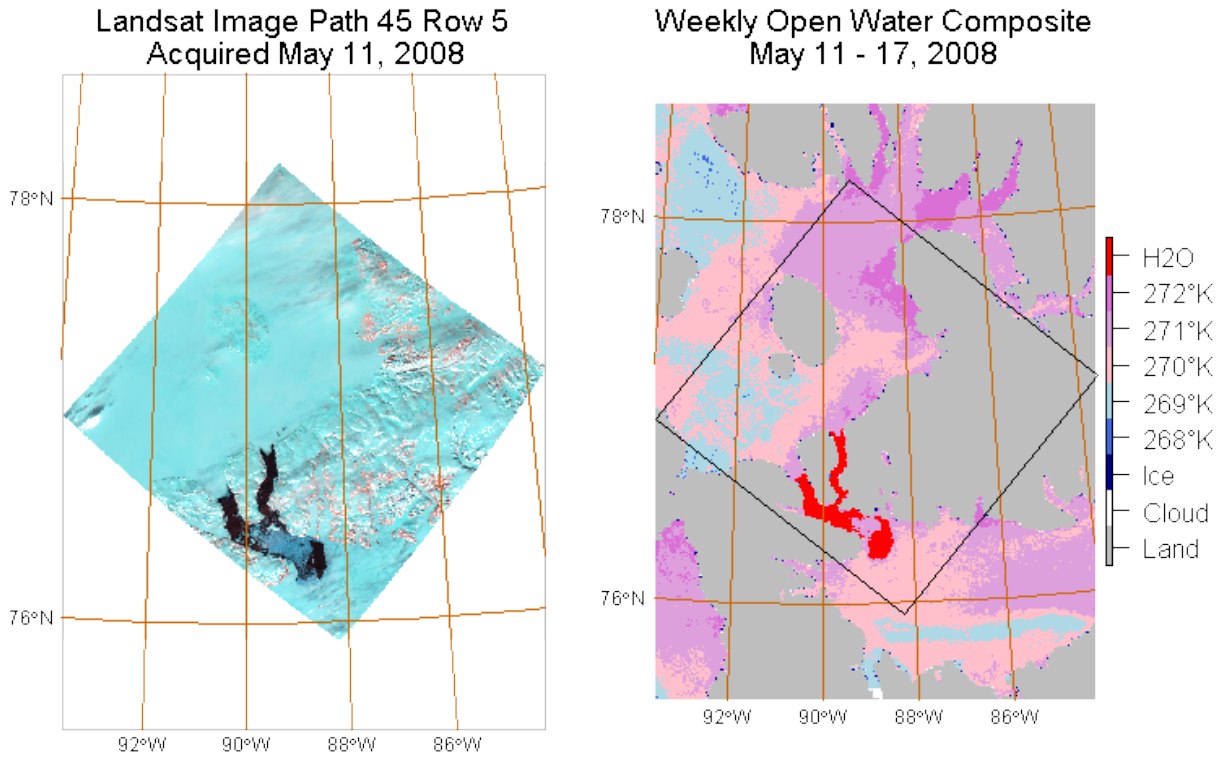

Figure 38: Landsat Comparison - Hell Gate May 11,2008

The next figure shows the same feature two weeks later on May 27, 2008. The polynya has grown to encompass most of North Kent Island and the classified result closely matches the Landsat scene.

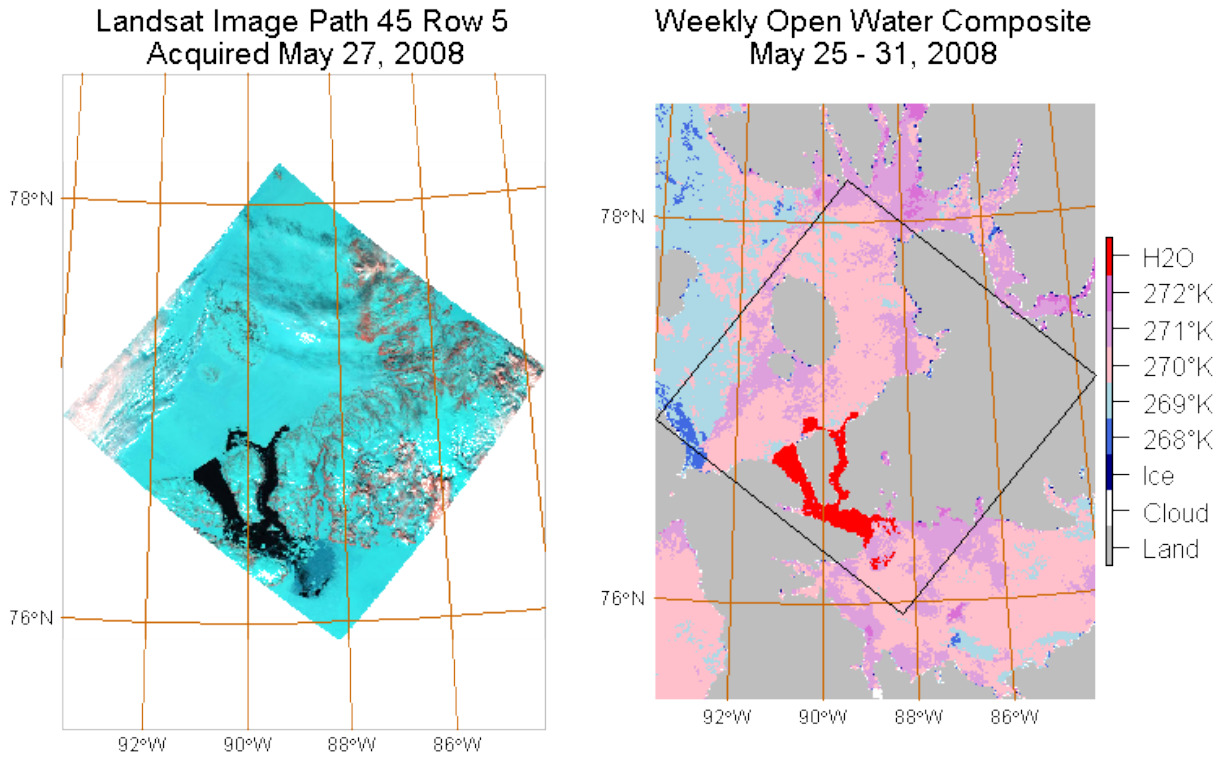

Figure 39: Landsat Comparison - Hell Gate May 27,2008

The next image shows the same feature twelve days later on June 8, 2008. Even though the Landsat image is mostly cloud covered, the open water areas are discernible as dark spots, which correspond well with the classified result.

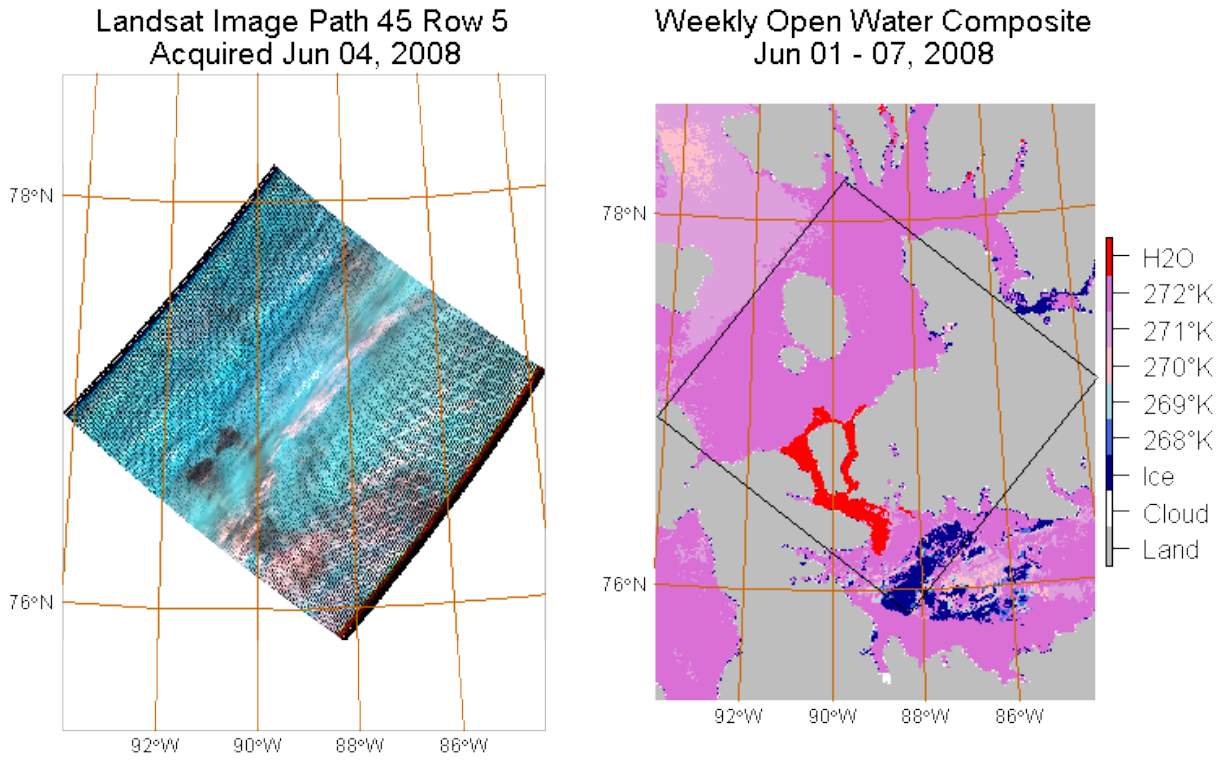

Figure 40: Landsat Comparison - Hell Gate June 8, 2008

Finally, the same location is seen on June 28, 2008.

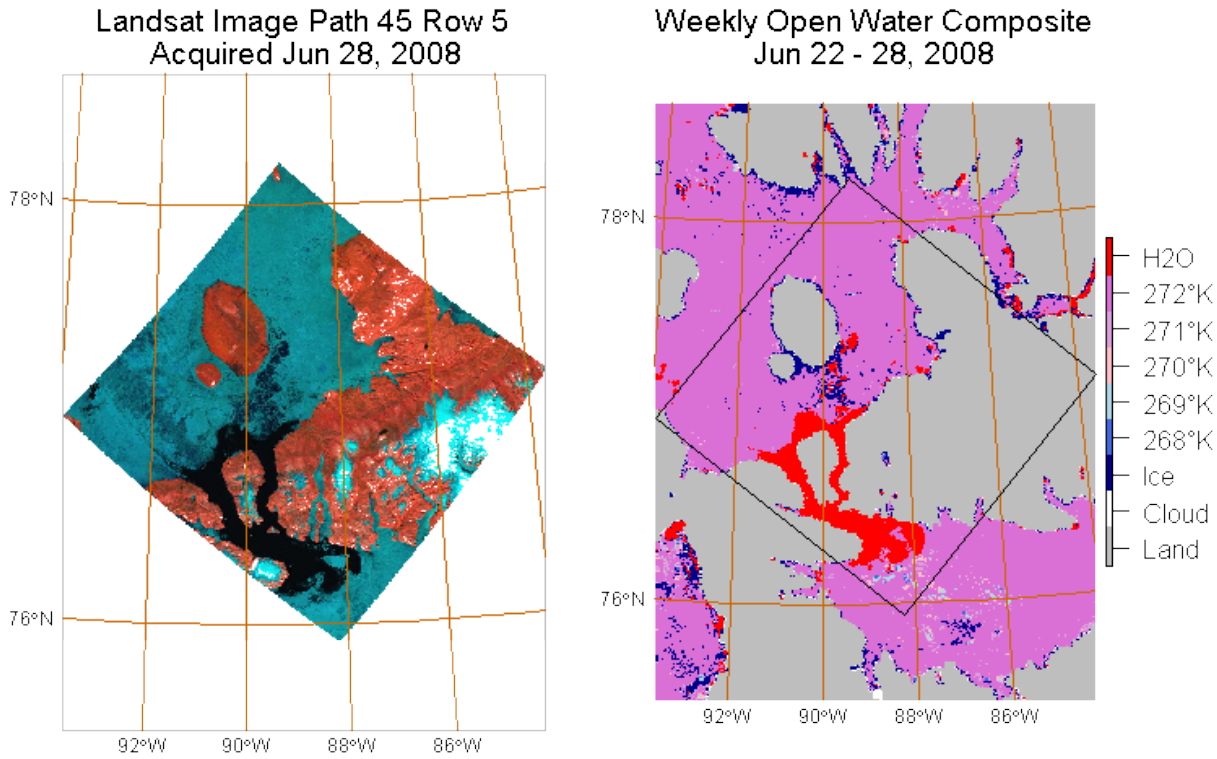

Figure 41: Landsat Comparison - Hell Gate June 28,2008

Analyzing the fraction of open water during specific weeks provides some insight into how the polynya size varies. Figure 42 shows the weekly open water fraction for the Hell Gate polynya over the project time frame, with the week beginning May 5th highlighted in red.

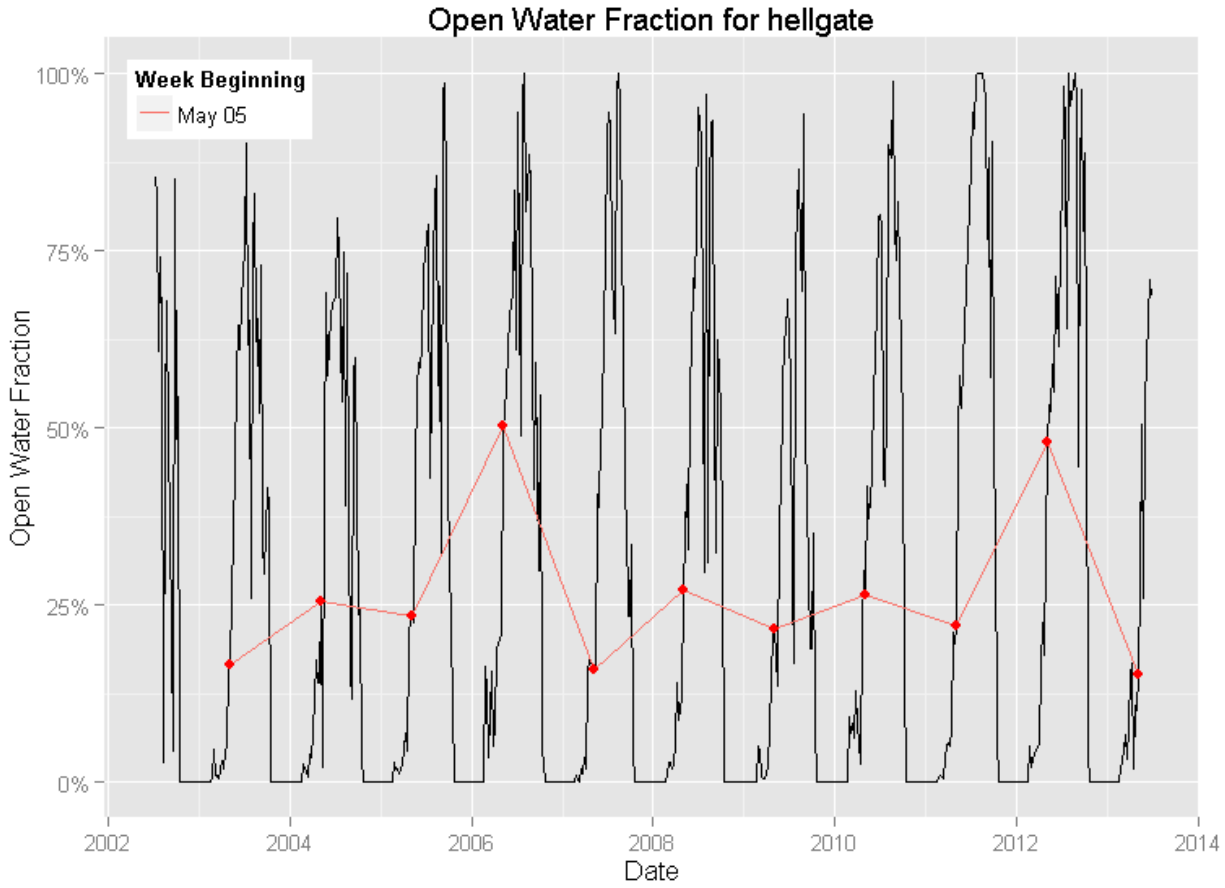

Figure 42: Spring Open Water Fraction Variation By Year - Hell Gate

Due to the much smaller size of the area being analyzed, and the fact it is centered on a known polynya, the open water fractions are much more variable than those calculated for the last ice area, exceeding 75% during the summer months. The graph also exhibits recurring observations of zero open water cells during the winter months. This situation highlights the major source of uncertainty resulting from using a passive sensor such as MODIS, which is the inability to penetrate cloud. In this case there is a strong likelihood that open water areas are obscured by cloud and fog.

Looking at the line for the week of May 5, the maxima occur in 2006 and 2012, while 2002, 2007 and 2013 represent the minima. The following figures illustrate the weekly open water composites for two years, with the area used for the analysis outlined in green.

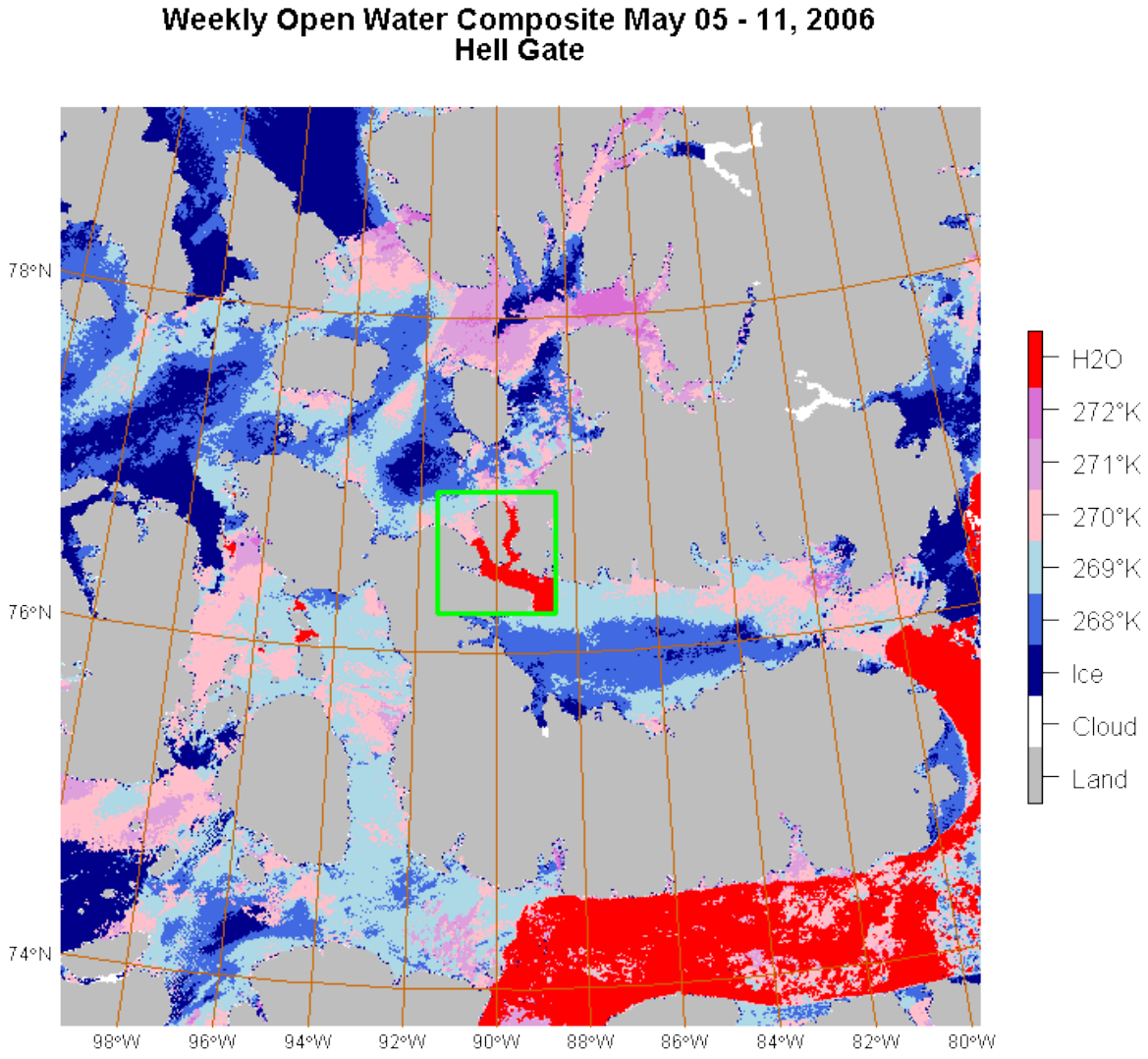

Figure 43: Weekly Open Water Composite - Hell Gate - May 5, 2006: This figure illustrates the distibution of open water detected in a year with the highest open water fraction relative to other years in the study. The green rectangle indicates the extent of the area used to compute the statistics shown in the previous figure.

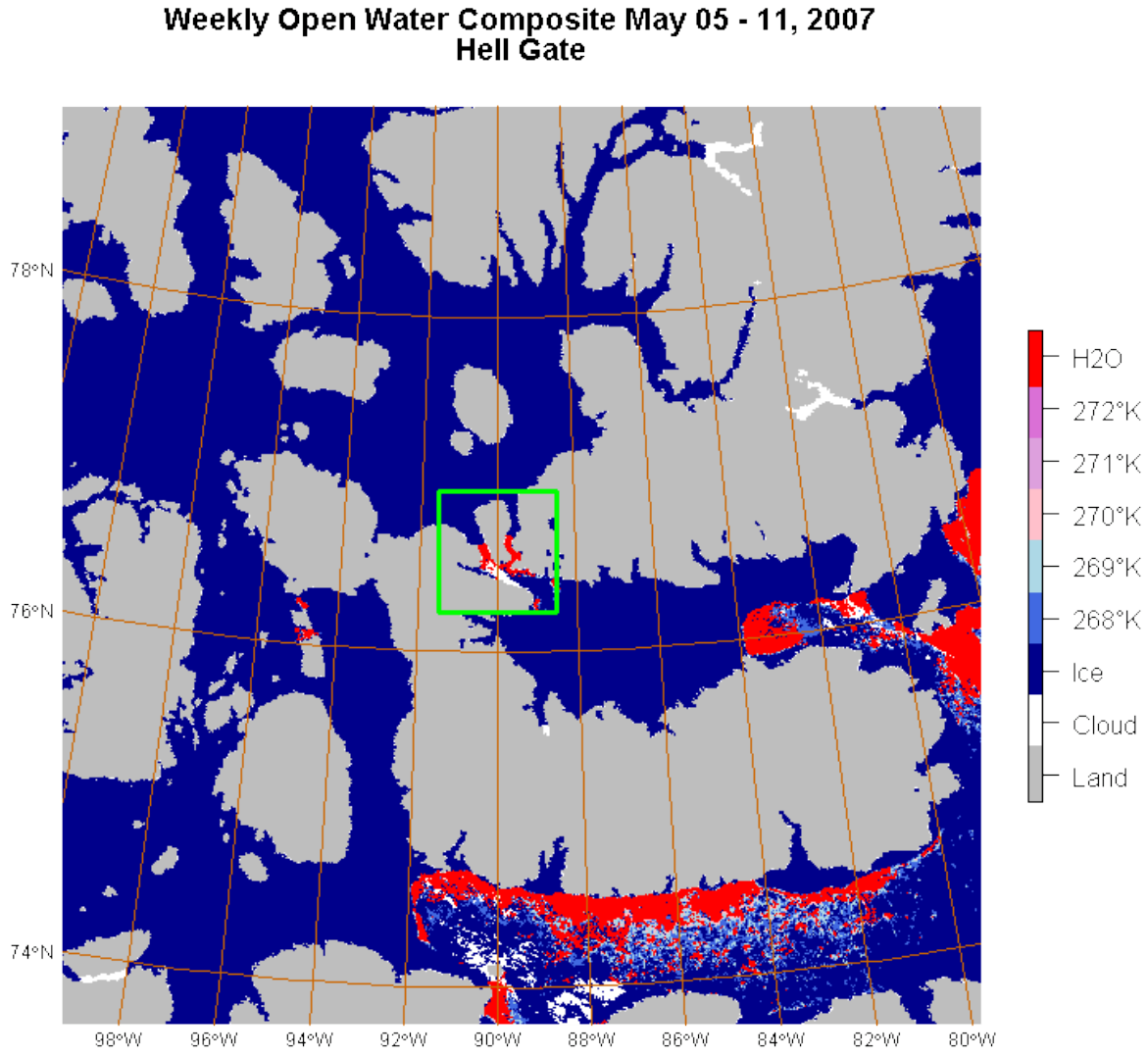

Figure 44: Weekly Open Water Composite - Hell Gate - May 5, 2007: As with the previous figure, this figure illustrates the open water occurrence in a year with low open water fractions. Note that a significant amount of cloud within the Hell Gate region outlined in green.

Once again, a considerable difference is observed in polynya extent and the presence of warmer ice on May 05, 2006 than the same week of 2007. However it is important to note the large amount of cloud (shown in white) in the 2007 data.

Summary

This study utilized MODIS Sea ice temperature grids to map potential polynya locations and extent in the Canadian Arctic and Northwest Greenland using satellite imagery collected up to four times daily over an eleven year time span. Even with the high imaging frequency afforded by a wide area sensor in polar orbit, there are considerable data gaps resulting primarily from cloud and to a lesser extent technical issues. A nearly continuous geographic coverage of the project area was obtained by classifying and aggregating the grids over seven day periods, using a filter biased towards open water detection.
Analyzing the resulting open water occurrence grids, we can calculate a spatial probability of occurrence distribution which closely matches previous maps of recurring polynyas during the early spring period.
Variation between years is evident, with extensive polynya growth observed in the spring during the years 2006 and 2010, however no obvious trends are apparent over the 2002-2013 time frame, and the early appearance of large polynyas does not appear to be predictive of more extensive melting later in the season. Given the length of the time period analyzed and the size of the area, it is possible that many subtle trends exist in the data but more intense scrutiny is required to discern them.
The quality of the result is affected by cloud, melt ponds, and coarse land masks which may limit the utility for near shore polynyas. For most locations, the result provides a useful open water grid with a spatial resolution of one kilometer and a temporal resolution of one week.

Recommendations

- Further validation using RADARSAT or ENVISAT imagery
- Additional insights may be possible by incorporating microwave radiometer data
- The current results provide a finely detailed history of the open water events in the Canadian Arctic and Northwest Greenland over the past eleven years. One well known polynya was briefly examined and some summary statistics have been prepared, however there are many targets within the data that would likely reward a deeper investigation.

References

“The impact and importance of production in polynya to top-trophic predators: three case histories Karnovsky, N., Ainley, D.G., and Lee, P. in Polynyas, Windows to the world eds Smith, W.O. Jr., & Barber, D. G. Elsevier Amsterdam 2007 (p. 392)”

“Meltofte, H. (ed) 2013. Arctic Biodiversity Assessment, Status and trends in Arctic biodiversity. Conservation of arctic Flora and Fauna, Akureyri.”

“Tynan, C.T., & DeMaster D. P. Observations and Predictions of Arctic Climatic Change: Potential effects on Marine Mammals, Arctic, Vol 50 No. 4 Dec. 1997 pp 308-322”

"Christie P., Sommerkorn M. 2012. RACER Rapid Assessment of Circum-Arctic Ecosystem Resilience, 2nd Ed. Ottawa, Canada, WWF Global Arctic Programme 72p."

"WMO - No.259 Suppl.No.5, 2010 - World Meteorological Organization Sea-Ice Nomenclature"

"Hall, D.K., J. Key, K.A. Casey, G.A. Riggs and D. Cavalieri, 2004: Sea ice surface temperature product from the Moderate Resolution Imaging Spectroradiometer (MODIS), IEEE Transactions on Geoscience and Remote Sensing, 42:1076-1087. "

"Clappa, Achille, and Giorgio Budillon. 2012. The Terra Nova Bay (Antarctica) Polynya Observed By modis ice Surface Temperature Imagery from May to June 2009. International Journal of Remote Sensing 33, no. 14: 4567-82."

"Hannah, C., Dupont, G., Dunphy, M., F., 2009. Polynyas and tidal currents in the Canadian Arctic Archipelago. Arctic 62, 83-95."

"Ice Navigation in Canadian Waters, 2013 Canadian Coast Guard"

"Canadian Ice Service (2011). Sea Ice Climatic Atlas for the Northern Canadian Waters 1981-2010, Environment Canada. [Online]"

"Smith, W and Barber, D ed, 2007. Polynyas: Windows To The World 1st Ed, Elsevier Science "

"Markus, T. and B.A. Burns. 1995. A method to estimate sub-pixel-scale coastal polynyas with satellite passive microwave data. J. Geophys. Res., 100(C3), 4473-4487.""

Appendix A: MODIS Sea Ice Products User Guide to Collection 5, 2006 Hall, D.K., et al

Appendix B: Weekly Open Water Composite Grids 2002-2013

Appendix C: Empirical Probability of Open Water Grids 2002-2013

Appendix D: Comparison with Landsat Quicklooks

Appendix E: Spatial Variation of EPO by Year